Author Manuscript
Author Manuscript
Author Manuscript
Author Manuscript

HHS Public Access
Author manuscript
*Cell*. Author manuscript; available in PMC 2024 February 05.

Published in final edited form as:
*Cell*. 2023 November 09; 186(23): 5114–5134.e27. doi:10.1016/j.cell.2023.09.024.

# Human MCTS1-dependent translation of JAK2 is essential for IFN-γ immunity to mycobacteria

*A full list of authors and affiliations appears at the end of the article.*

## Abstract

Human inherited disorders of IFN-γ immunity underlie severe mycobacterial diseases. We report X-linked recessive MCTS1 deficiency in men with mycobacterial disease from kindreds of different ancestries (from China, Finland, Iran, and Saudi Arabia). Complete deficiency of this translation re-initiation factor impairs the translation of a subset of proteins, including the kinase JAK2 in all cell types tested, including T lymphocytes and phagocytes. JAK2 expression is sufficiently low to impair cellular responses to IL-23 and partially IL-12, but not other JAK2-dependent cytokines. Defective responses to IL-23 preferentially impair the production of IFN-γ by innate-like adaptive MAIT and γδ T lymphocytes upon mycobacterial challenge. Surprisingly, the lack of MCTS1-dependent translation re-initiation and ribosome recycling seems to be otherwise physiologically redundant in these patients. These findings suggest that X-linked recessive human MCTS1 deficiency underlies isolated mycobacterial disease by impairing JAK2 translation in innate-like adaptive T lymphocytes, thereby impairing the IL-23-dependent induction of IFN-γ.

## One-Sentence Summary:

X-linked recessive human MCTS1 deficiency underlies mycobacterial disease by impairing JAK2 translation in innate-like T lymphocytes, thereby decreasing the IL-23-dependent production of IFN-γ by these cells upon mycobacterial challenge.

This work is licensed under a Creative Commons Attribution 4.0 International License, which allows reusers to distribute, remix, adapt, and build upon the material in any medium or format, so long as attribution is given to the creator. The license allows for commercial use.

[@]Correspondence: jonathan.bohlen@institutimagine.org (lead author), correspondence can also be directed to jacinta.bustamante@inserm.fr or casanova@rockefeller.edu.
[#,°,§,*]Equal contributions

Author Contributions

J.Bo., J.Bu., Q.Zha. and J.-L.C. conceived the study, designed the experiments, interpreted the data, and drafted the manuscript. J.Bo., Q.Zho., Q.Zha., C.C., Y.S., A.C., and L.A. analyzed WES data. J.Bo, Q.Zho., M.R. Q.P., J.R., M.O., A.-L.N., C.A.A.F., A.S.LH., L.E., J.E.H., C.Sc., C.So., T.L.-V., M.E., M.M., M.R., M.S., N.M., T.K., T.V., D.B., A.E., R.Y., A.Y., J.Pe., J.Pu., M.M.-V., M.M.-F., F.S., V.B., S.B-D., and Z.J., performed experiments and generated figures. S.S., E.S., M.A-S., G.E.G., N.Y., T.N., S.H., M.S., N.P., N.R., X.W., Q.Zha., and J.Bu. recruited patients and coordinated the clinical study protocol and sample collection. J.Bo., M.O., P.Z., and D.R. analyzed RNA-seq experiments. S.B.-D., A.T., J-.L.C., Q.Zha., and J.Bu. supervised experiments or analyses. All the authors discussed, revised, and approved the manuscript.

**Publisher's Disclaimer:** This is a PDF file of an unedited manuscript that has been accepted for publication. As a service to our customers we are providing this early version of the manuscript. The manuscript will undergo copyediting, typesetting, and review of the resulting proof before it is published in its final form. Please note that during the production process errors may be discovered which could affect the content, and all legal disclaimers that apply to the journal pertain.

Declaration of interests

J.-L.C. serves on the scientific advisory boards of ADMA Biologics Inc., Kymera Therapeutics, and Elixiron Immunotherapeutics.

Author Manuscript Author Manuscript Author Manuscript Author Manuscript

## Graphical Abstract

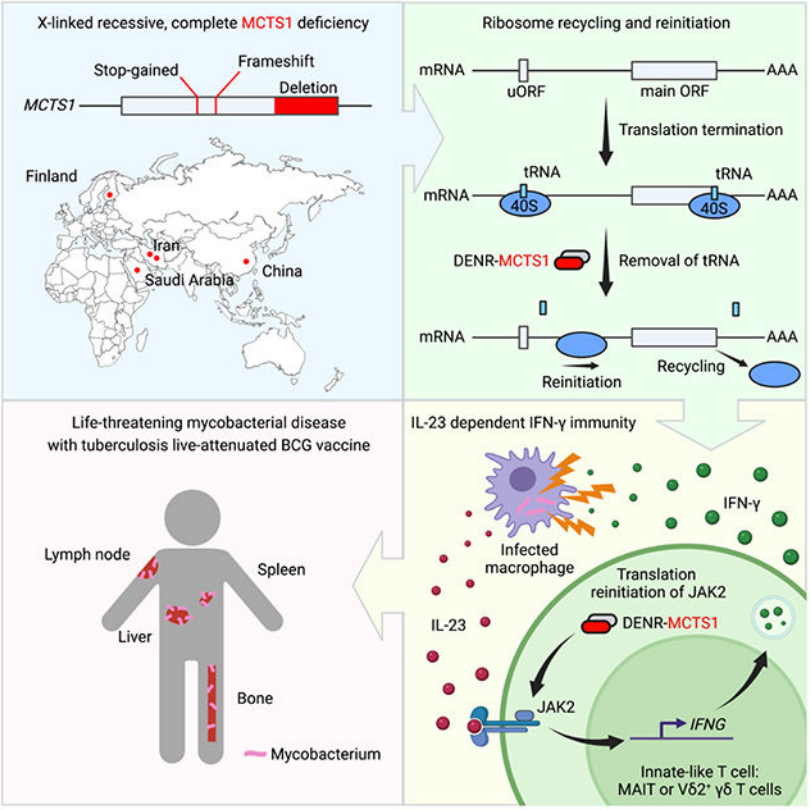


### Keywords

MCTS1; translation reinitiation; JAK2; IL-23; mycobacterium; MSMD; inborn error of immunity; X-linked disease

## Introduction

The clinical outcome of any infection varies considerably between individuals, ranging from silent infection in most, to lethal disease in a few[1,2]. Tuberculosis (TB), caused by *Mycobacterium tuberculosis*, has been a deadly infectious disease, with at least one billion deaths in the last 2,000 years[3]. However, infection with *M. tuberculosis* is silent or benign in >90% of infected individuals[3]. Forward genetics studies of rare patients with clinical disease due to the weakly virulent Bacillus Calmette–Guérin (BCG) live-attenuated vaccine against TB, or atypical environmental mycobacteria (EM) led to the discovery of human genetic and immunological determinants of TB[4–8]. Severe disease due to BCG or EM[9] in otherwise healthy individuals, particularly those without HIV infection or immunosuppression, is referred to as Mendelian susceptibility to mycobacterial disease (MSMD) because of the frequent occurrence of multiplex families and parental consanguinity[10]. MSMD is relatively rare, occurring in ~1 in 50,000 individuals[11,12], and is typically 'isolated' (~75% of cases) or, rarely, 'syndromic' (~25%)[12–14]. Patients with isolated MSMD are otherwise healthy and

Author Manuscript Author Manuscript Author Manuscript Author Manuscript

normally resistant to most common microbes, except, occasionally, other intramacrophagic pathogens, including some bacteria (e.g. *Salmonella*), fungi (e.g. *Coccidioidomyces*), and parasites (e.g. *Leishmania*)12.

Over the last 25 years, the discovery of inborn errors of interferon-gamma (IFN-γ) immunity has defined the root cause and immunological mechanism of MSMD and TB[11,14,16]. With one possible exception (ZNFX1 deficiency), all genetic defects underlying both isolated and syndromic MSMD perturb IFN-γ immunity (germline mutations of genes encoding IFN-γR1, IFN-γR2, IFN-γ, STAT1, IRF1, JAK1, IL-12Rß1, IL-12Rß2, IL-23R, IL-12p40, TYK2, SPPL2A, IRF8, NEMO, CYBB, ISG15, USP18, RORγT, and T-bet)[4–8,15,17–37]. Many genetic defects directly impair the production of IFN-γ, or the response to this cytokine (IFN-γR1, IFN-γR2, JAK1, STAT1, IRF1), whereas others affect the production of, or response to the IFN-γ-inducing cytokines IL-12, IL-23, and ISG15 (IL-12Rß1, IL-12Rß2, IL-23R, IL-12p40, TYK2, ISG15). Deficiencies of the IL-12-specific IL-12Rß2[30] and IL-23-specific IL-23R[30,41,42] also underlie MSMD, suggesting that neither of these two IFN-γ-inducing cytokines is dispensable for antimycobacterial immunity.

Human genetic studies of MSMD have, thus, revealed that IL-12- and IL-23-dependent IFN-γ immunity is essential for host defense against weakly virulent mycobacteria. Upon infection with mycobacteria[43], macrophages produce IL-12 and IL-23, which stimulate natural killer (NK) and T lymphocytes to produce IFN-γ. Several lymphocyte subsets have been identified as critical producers of IFN-γ and mediators of antimycobacterial immunity: patients with autosomal recessive (AR) SPPL2A or RORγT deficiency, or with autosomal dominant (AD) IRF8 deficiency suffer from MSMD due to a lack of T-helper ($T_H$) 1* cells[27,31], whereas AR T-bet deficiency impairs the development and IFN-γ production of NK cells, innate-like adaptive lymphocyte subsets (mucosal-associated invariant T cells [MAIT], Vδ2$^+$ γδ T, and invariant natural killer [iNKT] cells), and $T_H$1 cells[34]. In IL-12Rß1-, IL-12Rß2-, and IL-23R-deficient patients, these subsets (NK, MAIT, Vδ2$^+$ γδ T, iNKT, $T_H$1 and $T_H$1*) also fail to produce IFN-γ in response to IL-12 and/or IL-23[30,42]. IFN-γ can stimulate most cell types, but is crucial for the killing of mycobacteria within phagocytes[43,44], and it also boosts the production of IL-12 and IL-23 by these cells, forming a positive feedback loop[45–48].

Molecular genetics studies of MSMD have revealed the mechanisms of antimycobacterial immunity in humans *in natura*[9,49,50], demonstrating that IFN-γ acts as a key antimycobacterial cytokine rather than an antiviral interferon. Severe viral diseases are rare in patients with MSMD, occurring mostly in patients with syndromic MSMD who also have impaired IFN-α/β immunity (mutations of *JAK1, STAT1*, *TYK2*)[21,22,28,52]. Moreover, the study of MSMD has led to the discovery of both rare and common determinants of clinical TB, which is caused by *M. tuberculosis*, a bacterium 1,000 times more virulent than those implicated in MSMD[2]. Most genetic etiologies of MSMD have incomplete penetrance for MSMD and can manifest as genetic etiologies of TB[2,16,35]. Moreover, homozygosity for the common P1104A allele of TYK2 selectively impairs the IL-23-dependent induction of IFN-γ and accounts for about 1% of cases of TB in patients of European descent[2,18,54]. The study of MSMD has, therefore, had both biological and medical implications. However, a clear genetic etiology has yet to be found for about half the MSMD patients identified to

Author Manuscript Author Manuscript Author Manuscript Author Manuscript

date, implying that our understanding of antimycobacterial immunity is incomplete. In this context, we searched for new genetic causes and immunological mechanisms of MSMD.

## Results

### Hemizygosity for pLOF variants of MCTS1 in five unrelated men with MSMD

We hypothesized that MSMD might be due to the X-linked recessive (XR) inheritance of a single genetic defect in at least some patients in a cohort of patients with unexplained MSMD, as men outnumber women in this cohort (422 men, 359 women). We used whole-exome sequencing (WES) to search for rare predicted loss-of-function (pLOF, meaning stop-gain, frameshift, essential splice-site and large insertion/deletion) variants present on the X chromosome. We identified five independent, private (detected only in these kindreds) pLOF variants of the *MCTS1* gene in male patients from five kindreds (Figure 1A–B). Sanger sequencing confirmed the presence and familial segregation of these variants, consistent with the XR inheritance of MSMD (Figure 1A, Figure S1A–E). The enrichment of these *MCTS1* pLOF variants in our male MSMD cohort without genetic diagnosis ($n$ = 422, 5 pLOF variants) relative to a cohort comprising both male patients without mycobacterial infections and healthy male individuals ($n$ = 1,932, 0 pLOF variants) was highly significant ($p$ = 0.00013). The five patients come from unrelated, non-consanguineous families (Figure 1A, Case reports, Table S1). The patients are Chinese (P1), Finnish (P2), Saudi Arabian (P3), and Iranian (P4, P5) and are of East Asian, Finnish, Semitic, and Indo-European ancestries, respectively (Figure S1F). All patients were vaccinated with BCG within a day of birth (Table S1). The patients developed life-threatening BCG disease three months to one year after vaccination. Disease was multifocal or disseminated in several cases (P1-P3, P5), and involved osteomyelitis in P1 and P3. P1 died from BCG disease at the age of two years. The maternal uncle of P5 (P6) died at the age of two years from a condition consistent with MSMD (no genetic material available). P2, P3, P4, and P5 survived BCG infection and are now healthy at the ages of 18, 12, 6 and 3 years, respectively. There was no history of any other unusually severe infectious or non-infectious disease in these patients, suggesting a diagnosis of isolated MSMD. The brother of P5 (P7) was born in 2021, and was diagnosed as hemizygous for the familial *MCTS1* variant six days after birth; BCG vaccination was, thus, contraindicated, and he remains asymptomatic to date. Detailed clinical reports are provided in the methods section. These cases highlight the potential role of *MCTS1* variants in isolated MSMD.

### pLOF variants of MCTS1 and DENR are absent from the general population

All five pLOF variants of the *MCTS1* gene identified in the five index patients are private, with combined annotation-dependent depletion (CADD) scores well above the mutation significance cutoff (MSC) for *MCTS1*[55,56] (Figure 1C), further suggesting that they are deleterious. No pLOF variant of *MCTS1* in the hemizygous, homozygous, or heterozygous state was reported in the gnomAD dataset (v2, 125,748 whole-exome and 15,708 whole-genome sequences). Ten missense variants of *MCTS1 (ENST00000371317)* in the hemizygous state are reported in gnomAD (Figure 1C). A search of our in-house WES and WGS (whole-genome sequencing) datasets from more than 15,000 individuals with various infectious diseases revealed no additional hemizygous pLOF variants of

Author Manuscript Author Manuscript Author Manuscript Author Manuscript

*MCTS1*. The probability of *MCTS1* being loss-of-function-intolerant (pLI) was found to be 0.87, indicating that truncating variants are not tolerated in the general population. Density-regulated re-initiation and release factor (DENR) is the constitutive binding partner of MCTS1, and these two proteins are interdependent for ribosome recycling and re-initiation activity (Figure 1D)[58,59]. DENR knockout (KO) and MCTS1 knockdown (KD) are lethal during the development of *Drosophila melanogaster* because they impair histoblast proliferation[58]. No studies of DENR$^{KO}$ mice or MCTS1$^{KO}$ animal models have yet been published, but International Mouse Phenotyping Consortium (IMPC) data suggest that DENR$^{KO}$ is embryonically lethal in mice, whereas MCTS1$^{KO}$ mice are viable and have no obvious phenotype[60] (the DENR and MCTS1 KO phenotypes are summarized in Table S2). DENR pLOF variants are very rare in gnomAD, with a cumulative allele frequency of $5.5*10^{-5}$ and no homozygous carriers detected. We found no individuals heterozygous or homozygous for pLOF variants of *DENR* in our own cohort of patients with various infectious diseases, including MSMD. Collectively, these data suggest that the hemizygous pLOF variants of *MCTS1* identified in these patients from five unrelated kindreds probably underlie their MSMD.

## The patients' variants are loss-of-expression (LOE)

*MCTS1* (ENSG00000232119, ENST00000371317.10) encodes malignant T cell-amplified sequence 1, a 181-amino acid polypeptide composed of a domain of unknown function (DUF1947) and an RNA-binding domain (PUA) (Figure 1B). P1's variant (c.225_226insG) causes a frameshift resulting in a premature stop codon (p.P77Afs*22, Figure 1B). P2's variant (c.213dupT) creates a premature stop codon (p.R72*). The variant found in P3 (c.164+1_164+4delGTAA) is predicted to disrupt the consensus sequence for the splicing donor site of *MCTS1* intron 2. Indeed, exon trapping in COS-7 cells and the sequencing of whole-blood RNA from P3 and his parents confirmed a severe impairment of splicing at this site, with no production of the canonical transcript in COS-7 cells (Figure S2A) and less than 3% of reads supporting normal splicing in P3's blood (Figure S2B, C). In more than 90% of splicing events, exon 2 is skipped, resulting in a truncated MCTS1 protein lacking the 51 amino acids encoded by exon 2 (p.K4_C55delinsN). The residual splicing events skip both exon 2 and exon 3 or retain intron 2, leading, in both cases, to a frameshift and the gain of a premature stop codon. Finally, the *MCTS1* alleles of P4, P5 and P7 present two different large deletions (4,128 and 5,619 nucleotides) affecting the two exons at the 3'-end of *MCTS1* (P4: g.120610122_120614250del; P5 and P7:g.120610241_120615860delinsCAT) (Figure S2D). Both lead to predicted truncation of the MCTS1 protein (p.A133_K181del). We assessed protein production for the patients' *MCTS1* variants. We transiently transfected MCTS1$^{KO}$ HeLa cells[59] with wildtype (WT) or variant *MCTS1* cDNA constructs and assessed MCTS1 protein levels by western blotting (Figure 2A). None of the five *MCTS1* alleles found in MSMD patients drove the expression of a full-length or truncated MCTS1 proteins, whereas all the missense *MCTS1* variants found in gnomAD drove MCTS1 expression. We also observed a lack of MCTS1 production and low levels of DENR protein in the primary fibroblasts of P2 (Figure 2B), T-cell blasts (T-blasts) from P2, P4, P5, and P7 (Figure 2C), and primary neutrophils from P2 (Figure 2D). The heterozygous female carriers tested — the sister and mother of P2 — and the wild-type father of P2, had normal levels of MCTS1 protein in primary neutrophils (Figure 2D). Thus, none of the *MCTS1* variants

Author Manuscript Author Manuscript Author Manuscript Author Manuscript

encodes a detectable MCTS1 protein when overexpressed in recipient cells or in primary hemizygous cells.

## The patients' variants are loss-of-function for translation re-initiation

*MCTS1* and *DENR* are ubiquitously expressed in all cell types and tissues in humans[61]. Following the translation of an open-reading frame (ORF) by a ribosome, the DENR-MCTS1 complex removes the tRNA from the 40S ribosome on the stop codon, as a part of ribosome recycling (Figure 1D). In eukaryotic cells, there are at least two types of ORFs: classical, protein-coding ORFs (main ORFs, mORF) and upstream ORFs (uORF), which are small coding sequences in the 5'UTR of mRNAs. These uORFs occur in about half of all mammalian mRNAs and downregulate the translation of mORFs[60]. We hypothesized that XR MCTS1 deficiency might disturb ribosome recycling at two types of stop codons: classical mORF and 5'UTR uORF stop codons. We first assessed MCTS1 function on uORF stop codons, for which MCTS1 promotes the re-initiation of translation[58,59]. In the absence of MCTS1 or DENR, 40S ribosomes stall on the uORF stop codon, because the deacylated tRNA cannot be removed[59]. This has a roadblock-like effect, leading to poor expression of the corresponding mORF of the mRNA, due to impaired translation re-initiation. We assessed the five *MCTS1* LOE mutations in a luciferase-based translation re-initiation assay (Figure 2E). This assay uses a reporter plasmid with a short uORF in its 5'UTR, rendering expression of the reporter gene dependent on the MCTS1-DENR complex[58,59]. The *MCTS1* variants found in MSMD patients were loss-of-function (LOF) for MCTS1 activity (Figure 2F), like the synthetic A109D LOF mutation used as a negative control[62]. All 16 non-synonymous variants found in the general population were tested and found to have activity levels similar to those of the (WT) MCTS1 (isomorphic variants). *MCTS2P* is an *MCTS1* paralog and pseudogene located on a different chromosome (Chr. 20). The predicted protein sequence of MCTS2P is ~95% identical to that of MCTS1 (Figure S2E). In our functional assay, MCTS2P had detectable but weak activity with the DENR-MCTS1-dependent reporter (Figure S2I). However, queries against all the RNA-sequencing datasets produced in this manuscript showed that none of the total of 4.7 billion reads mapped uniquely to *MCTS2P*, whereas 403,296 reads mapped to *MCTS1* (Figure S2F–H). Consistently, CAGE data from the FANTOM5 project suggest that the *MCTS1* promoter is much stronger (score 33.8) than the putative *MCTS2P* promoter (score 0.69)[63,64]. These data suggest that *MCTS2P* is a non-functional paralog of *MCTS1*, due to its lack of transcription. Collectively, these results suggest that the *MCTS1* variants found in the MSMD patients from the five unrelated kindreds abolish MCTS1 reinitiation activity, resulting in complete MCTS1 deficiency.

## Ribosomal recycling is impaired in the patients' cells

We hypothesized that cells lacking MCTS1 might display ribosome recycling defects. We tested this hypothesis by performing 40S and 80S ribosome footprinting (Figure S3A) on $MCTS1^{KO}$ and WT HeLa cells (Figure S3B–D)[59,65,66]. This method reveals the position and number of 40S and 80S ribosomes on endogenous mRNAs[65,66]. We found that the frequency of stalled, post-termination 40S ribosomes was higher on mORF stop codons in $MCTS1^{KO}$ cells (Figure 3A, indicated by arrow), as in $DENR^{KO}$ HeLa cells, although the 40S peak for $MCTS1^{KO}$ was smaller[59]. This finding is consistent with MCTS1 deficiency,

Author Manuscript Author Manuscript Author Manuscript Author Manuscript

as post-termination 40S ribosomes are the substrate of DENR-MCTS1. We observed 80S ribosome queueing in front of mORF stop codons (Figure 3B, indicated by an arrow), due to the translating 80S ribosomes running into the roadblock caused by the stalled 40S ribosome on the stop codon, as described in DENR$^{KO}$ HeLa cells and yeast strains lacking DENR or MCTS1[59,67] MCTS1$^{KO}$ HeLa cells, thus, have impaired ribosome recycling. We investigated whether cells from MCTS1-deficient patients had the same molecular phenotype. We used the same 40S and 80S footprinting method on SV40-fibroblasts from P2 stably transduced with lentiviral empty vector (EV) or a lentiviral vector encoding wildtype (WT) MCTS1 (Figure S3E–G). P2's SV40-fibroblasts had a pronounced peak of stalled post-termination 40S ribosomes on mORF (Figure 3C) and uORF stop codons (Figure S3H), which was rescued by transduction with WT *MCTS1*. The queueing 80S ribosomes in front of the stop codon were, therefore, also rescued by MCTS1 expression in P2's cells (Figure 3D). Furthermore, cells from P2 transduced with EV presented an accumulation of 40S ribosomes on mORF (Figure 3E) and uORF (Figure S3I) stop codons in the presence of certain penultimate (position −1 relative to the stop) codons, such as ATG$^{Met}$ and GCG$^{Leu}$, another phenocopy of DENR$^{KO}$ HeLa cells (Figure S3J–K). We have previously shown that this ribosome recycling defect does not negatively affect the translation of the proteins concerned[59]. The patients' cells, thus, display impaired ribosome recycling due to their lack of MCTS1, attesting to a deficiency of the two known functions of MCTS1.

## The patients' cells are defective for translation re-initiation

Translation may be re-initiated in almost half of all human genes[60]. The MCTS1-DENR complex is specifically required for translation re-initiation following uORFs that are either very short[58,62] or terminate in certain penultimate codons[59] (~200 of 8,900 detected genes[59]). We identified the genes poorly translated in MCTS1-deficient cells by comparing the translation efficiency of all detected genes ($n$ = 10,505) between P2 SV40-fibroblasts transduced with EV and with WT MCTS1 (Figure 3F). Xtail[68] analysis identified 26 genes as having significantly higher levels of translation after MCTS1 rescue in P2's cells (Figure 3F), with translation levels decreasing for only two genes following such rescue (Table S3). *JAK2* is the only target gene directly related to IFN-γ immunity, as JAK2 is required for the IL-12- and IL-23-dependent induction of IFN-γ and the response to IFN-γ[18,70]. Another affected gene important for cytokine signaling is *IFNAR1*, encoding a chain of the IFN-α/β receptor (Figure 3F). Patients with germline mutations of *IFNAR1* and related genes suffer from viral, but not mycobacterial disease[2]. We investigated the translational targets of MCTS1 in a more relevant cell type, by performing 80S ribosome footprinting in primary T-cell blasts from four healthy male individuals and four MCTS1-deficient patients (P2, P4, P5 and P7). We again found that many more genes had lower levels of translation (143 genes) in the patients' cells than had higher levels of translation (46 genes) (Figure 3G). We observed a substantial and significant overlap ($n = 98$, $p < 10^{-20}$) between the DENR-dependent genes identified in DENR$^{KO}$ HeLa cells ($n = 275$, $p < 0.1$) and the MCTS1-dependent genes in identified in MCTS1-deficient T-cell blasts ($n = 297$, $p < 0.1$) (Figure S3L, Table S4). The cells of MCTS1-deficient patients, like DENR$^{KO}$ cells, therefore have a genome-wide translation re-initiation defect. *IFNAR1* was also affected, as in SV40-fibroblasts (Table S5). JAK2 translation levels were less than half those in wild-

Author Manuscript Author Manuscript Author Manuscript Author Manuscript

type cells (Figure 3G–H). We also assessed the translation efficiency of 25 genes related to IFN-γ immunity, including 16 of the 20 genes underlying MSMD endogenously expressed in these T-cell blasts; we found that only *JAK2* and *IRF8* were substantially affected in the patients' cells (Figure S3M). *IRF8* mRNA levels are upregulated in MCTS1-deficient patients (Figure S3N), potentially compensating for the lower efficiency of translation at mRNA level, whereas *JAK2* mRNA levels were unaffected. Altogether, the patients' cells presented defective translation re-initiation, resulting in the impaired translation of a subset of mRNAs, including that encoding JAK2.

## MCTS1-dependent translation re-initiation is required for JAK2 expression

We hypothesized that MCTS1 deficiency underlies MSMD by disrupting the translation of JAK2. We assessed the MCTS1-dependence of 17 genes underlying MSMD and other genes involved in IFN-γ immunity, including JAK2, by performing 5'UTR reporter assays in MCTS1$^{KO}$ HeLa cells (Figure 4A). For many of these genes, we tested multiple alternative 5'UTRs. A significant decrease, of more than 65%, was observed only for the JAK2 reporter, which was rescued by the re-expression of WT MCTS1 but not the patients' variants or the synthetic LOF allele A109D (Figure 4B). JAK2 reporter translation was also dependent on the presence of DENR (Figure S4A). We then investigated the molecular mechanism of the dependence of JAK2 translation on MCTS1. We identified three uORFs within the JAK2 5'UTR, two of which were ultra-short Start-Stop "stuORFs" (Figure 4C, Scheme of WT JAK2 5'UTR). Mutation of the uORFs within the JAK2 5'UTR revealed that the two stuORFs (uORFl and 2, but not uORF3) contributed to the MCTS1-dependence of this 5'UTR (Figure 4C). We also observed an accumulation of 40S ribosome footprints on both stuORFs in the endogenous JAK2 5'UTR (Figure 4D). We, thus, showed that the translation of JAK2, unlike that of 28 other genes related to IFN-γ immunity, was MCTS1-dependent. We then hypothesized that MCTS1 deficiency might impair JAK2 expression in MCTS1$^{KO}$ cell lines and patients' cells. CRISPR/Cas9-mediated knockout of MCTS1 in monocytic leukemia THP-1 cells caused a reproducible drop in endogenous JAK2 levels in five independent MCTS1$^{KO}$ clones (Figure 5A, Antibody validation: Figure S4B). JAK2 production was also decreased, but not abolished, in P2's SV40-fibroblasts, and this defect was rescued by transduction with WT MCTS1, but not with the patients' variants or A109D (Figure 5B). Patient-derived T-saimiri virus-transformed T cells (HVS-T) and T-cell blasts had four-fold lower levels of JAK2 (Figure 5C–D). The re-expression of MCTS1 by stable transduction rescued JAK2 levels both in patients' T-cell blasts (Figure S4C) and in MCTS1$^{KO}$ THP-1 cells (Figure S4D). Thus, MCTS1 deficiency caused a three- to five-fold decrease in JAK2 protein levels in the three cell types tested (Figure 5E).

## Normal presence and frequency of leukocyte subsets in MCTS1 patients

JAK2 is one of four members of the Janus kinase family involved in JAK-STAT signaling in response to more than 50 cytokines[71]. No complete or partial genetic deficiency of human JAK2 has ever been reported and JAK2 knockout is embryonically lethal in mice[70]. Given the major hematological alterations observed in humans with JAK3[72] deficiency (underlying SCID) and JAK2$^{KO}$ mice, we hypothesized that impaired JAK2 expression in MCTS1-deficient patients would lead to abnormal myeloid or lymphoid development. However, MCTS1-deficient patients had normal complete blood count (CBC) profiles

Author Manuscript Author Manuscript Author Manuscript Author Manuscript

(Table S1). We also performed deep, mass cytometry-based immunophenotyping on four MCTS1-deficient patients (P2, P4, P5 and P7). We found that all the subsets detected (Figure S5A–D), including IFN-γ-producing lymphocyte subsets (Figure S5B) and IL-12- and IL-23-producing monocytes and dendritic cells (DCs) (Figure S5C), were present at counts and frequencies (data not shown) in the range of age-matched controls. This suggests that MSMD in MCTS1-deficient patients is not mediated by an absence or low frequency of any particular leukocyte cell subset, consistent with the clinical phenotype of isolated, as opposed to syndromic MSMD.

### *MCTS1 deficiency impairs IFN-γ production upon BCG infection* in vitro

As one of the four JAK kinases, JAK2 mediates responses to three cytokines related to IFN-γ-mediated immunity — IL-12, IL-23, and IFN-γ — through its association with the IL-12Rß2, IL-23R, and IFN-γR2 receptor chains and the mediation of signal transduction after cytokine binding[73–75]. The 20 known JAK2-dependent cytokines and the phenotypes of humans with genetic variants resulting in a deficiency of one of these cytokines or the corresponding receptor are listed in Table S6. We hypothesized that MCTS1 deficiency might impair IFN-γ circuit activation (i.e. the relevant leukocyte function) in response to mycobacterial infection by decreasing JAK2 levels. We tested this hypothesis by infecting fresh whole-blood cells from healthy travel controls and MCTS1-deficient patients with BCG and measuring IFN-γ production after 48 hours. Whole blood from patients P2 and P5 contained IFN-γ levels 13-fold lower than those of healthy travel controls (Figure S5F). IFN-γ production was only partially rescued by co-stimulating the patients' cells with IL-12, suggesting that IL-12 is not the major contributor to this defect. The defect of IFN-γ production following stimulation with BCG alone was as profound as that in TYK2- and IL-12Rß1-deficient patients (Figure S5F). In summary, leukocytes from MCTS1-deficient patients have a severely impaired response to BCG infection *in vitro* in terms of IFN-γ production, despite their normal counts of cells from the lymphoid and myeloid subsets.

## Intact type I and type II interferon response pathways in MCTS1-deficient cells and blood from the patients

Based on the defective response of the patients' blood cells to BCG and the role of JAK2 in the response to IFN-γ[70], we hypothesized that the low JAK2 levels in the cells of MCTS1-deficient patients would impair their response to IFN-γ. However, we found that this was not the case. MCTS1$^{KO}$ THP-1 cells responded normally to IFN-γ stimulation, as measured by the induction of pSTAT1 (Figure S6A) and *IRF1* mRNA (Figure S6B, C). MCTS1$^{KO}$ THP-1 cells also displayed normal levels of STAT1 phosphorylation in response to IFN-α (Figure S6A). Transcriptome-wide pathway induction, detected by RNA-seq upon treatment with IFN-α and two doses of IFN-γ, was also intact in MCTS1$^{KO}$ THP-1 cells (Figure S6D). The response to IFN-γ was normal in terms of STAT1 phosphorylation, as shown by the western blot of SV40-fibroblasts from P2 (Figure S6E) as was the response to IFN-α, as shown by the induction of *MX1* mRNA (Figure S6F). We then investigated the response to IFNs in primary cells from the patients. We studied the response to IFN-γ and IFN-α2 in monocyte-derived macrophages (MDMs), monocyte-derived dendritic cells (MDDCs), and monocyte-derived osteoclasts (MOCs) for P2. These cells responded normally to both IFNs, as shown by assessments of STAT1 phosphorylation (Figure S6G–I). Moreover, MDMs from P2 had

Author Manuscript Author Manuscript Author Manuscript Author Manuscript

normal transcriptional responses, as shown by RNA-seq (Figure S6J). We also stimulated fresh blood from patients P4, P5, and four healthy controls with IFN-γ and IFN-α, and used mass cytometry to assess the induction of STAT phosphorylation. The induction of STAT1, STAT3, and STAT5 phosphorylation was generally similar in patients and controls following treatment with IFN-α or IFN-γ, in all peripheral leukocyte subsets studied (Figure S6K). Two conclusions can be drawn from these findings. First, the low levels of JAK2 observed in MCTS1-deficient cells are not sufficiently low to impair responses to IFN-γ, either in MCTS1-deficient cell lines or in primary cells from patients. Second, even though *IFNAR1* is a reproducible MCTS1 target in both patient-derived SV40-fibroblasts and T-cell blasts (Figure 3F, G), the response to IFN-α is intact in MCTS1-deficient cell lines and primary cells from the patients. This finding is consistent with the absence of severe viral infections in the five MCTS1-deficient patients (Case Reports in Methods Section), despite exposure to common viruses, as attested by positive viral serology results for P2 and P5 (Figure S6L, M, Table S7). The patients' cellular responses to IFN-γ and IFN-α were intact.

## Defective IL-23 and intact IL-12 response pathways in MCTS1-deficient cells

Given the intact cellular response to IFN-γ in the patients, we hypothesized that cellular responses to IL-12 and IL-23, which are also mediated by JAK2[73–75], might be impaired in MCTS1-deficient patients. We used primary T-cell blasts from the patients to assess cellular responses to IL-12. These cells responded normally to IL-12 stimulation, as assessed by measuring the induction of pSTAT4 (Figure S7A). Patient-derived HSV-T cells also responded normally to IL-12 through the induction of *IFNG* mRNA (Figure S7B). Patient-derived or isogenic IL-23-sensitive cells are not available, because T-cell blasts and HSV-T cells do not display robustly detectable STAT3 phosphorylation upon IL-23 treatment in long-term culture (Figure S7C). We assessed the response to IL-23 and IL-12 in T-cell blasts by transcriptome profiling. T-cell blasts from nine healthy individuals, four MCTS1-deficient patients, two patients homozygous for the hypomorphic P1104A TYK2 allele that selectively impairs responses to IL-23[18], and one patient each with autosomal recessive, complete TYK2, IL-12Rß1, and IRAK4 deficiencies were stimulated with IL-12, IL-23, IL-1ß, or IL-1ß plus IL-23 for 6 hours. We then performed RNA sequencing. We used IL-1ß as an IL-23-sensitizing agent, as previously described[35,42]. We found that MCTS1-deficient T-cell blasts responded normally to IL-12 and IL-1ß, but that their responses to IL-23 and to IL-23 plus IL-1ß were impaired (Figure 5G, Figure S7D). As MDMs apparently also respond weakly to IL-23 (Sun and Abraham, 2020) by inducing the expression of antimicrobial genes (e.g. p40phox and NOS2), we stimulated MDMs from three healthy controls and P2 with IL-23 for 6 hours. The response of MDMs from P2 to IL-23 was weak compared to healthy controls, as shown by pathway enrichment analysis on RNA-seq data, whereas these cells responded normally to IFNs (Figure S6J). Thus, the response to IL-12 was intact, whereas the response to IL-23 was impaired in the cells of MCTS1-deficient patients.

## Impaired JAK2 expression in MCTS1-deficient cells impairs cellular responses to IL-23

We then investigated whether the impaired response to IL-23 in MCTS1-deficient cells was due to low levels of JAK2 expression. We used a HEK-Blue IL-23 reporter cell line, in which the cells were stably transduced with IL-23R and a STAT3-dependent reporter

Author Manuscript Author Manuscript Author Manuscript Author Manuscript

gene. We produced polyclonal knockout lines for MCTS1 ($MCTS1^{KO}$) or JAK2 ($JAK2^{KO}$) by CRISPR/Cas9 gene editing (Figure S7E). The $MCTS1^{KO}$ HEK cells had ~50% the normal level of JAK2 protein (Figure S7F), a deficit smaller than that observed in the patients' cells (Figure 5E). As expected, $JAK2^{KO}$ HEK-blue cells had a strongly impaired response to IL-23 (Figure S7G). We also found that $MCTS1^{KO}$ cells had an impaired response to IL-23 at concentrations of both 1 ng/ml and 0.1 ng/ml (Figure S7G). We stably transduced these HEK-blue cells with a construct harboring an empty expression vector (EV) or a construct containing the MCTS1 coding sequence (M). MCTS1 overexpression rescued JAK2 expression in $MCTS1^{KO}$ cells but not in $JAK2^{KO}$ HEK-Blue cells (Figure 5G). Importantly, MCTS1 overexpression also rescued the impaired response to IL-23 of $MCTS1^{KO}$ HEK-Blue cells, whereas it increased the response to IL-23 only slightly in the other three lines (Figure 5H). These findings confirm that the impaired response to IL-23 is due to the lack of MCTS1. Finally, we stably transduced these four HEK-Blue lines with an empty expression vector (EV) or a construct encoding the JAK2 ORF (J2) under the control of an endogenous promoter for the production of moderate amounts of JAK2. This partially rescued JAK2 levels in $MCTS1^{KO}$ and $JAK2^{KO}$ HEK-Blue cells (Figure 5I). Importantly, JAK2 overexpression rescued the response to IL-23 in $MCTS1^{KO}$ and $JAK2^{KO}$ HEK-Blue cells (Figure 5J). These findings demonstrate that a lack of MCTS1 impairs cellular responses to IL-23 through decreases in JAK2 expression.

## Particular dependence of the IL-23 response pathway on JAK2

We investigated the possibility of the IL-23 response pathway being particularly sensitive to decreases in JAK2 levels or activity. We transfected JAK2-deficient γ2A-fibrosarcoma cells expressing IL-23R and IL-12Rβ1 with various amounts of JAK2-encoding constructs and assessed their response to IL-23. In this system, the levels of IL-23-dependent STAT3 phosphorylation were dependent on JAK2 levels (Figure S7H). Thus, low levels of JAK2 protein can impair cellular responses to IL-23. We then investigated the dependence of several cytokine response pathways on JAK2. We expanded primary sorted NK cells by culture with feeder PBMCs and IL-2. These cells had a high purity (>95%, Figure S7I) and responded robustly to IL-23 plus IL-1β, or to IL-12, by secreting IFN-γ (Figure S7J). We also isolated primary monocytes, which responded to stimulation with IFN-α and/or IFN-γ by producing IP-10, IL-12p70 and/or TNF (Figure S7K–M). The response to IL-23 or IL-12 is mediated by JAK2 and TYK2, whereas the response to IFN-γ depends on JAK1 and JAK2 and the response to IFN-α depends on JAK1 and TYK2[77]. By contrast, the response to IL-1β is JAK2-independent, and even entirely independent of JAK proteins. We investigated the dependence of these cytokine response pathways on JAK2, using increasing concentrations of gandotinib, a JAK2-specific inhibitor ($IC_{50}$ for JAK2=3nM, JAK1=19.8nM, TYK2=44nM, JAK3=48nM)[78]. We found that the response of NK cells to IL-23 + IL-1β was much more sensitive to gandotinib than the response to IL-12 (Figure 5K, Figure S7N). In monocytes, the responses to IFN-α and IFN-γ were as sensitive or less sensitive to gandotinib than the response to IL-12 (Figure 5K, Figure S7O,P,Q). Impaired or abolished cytokine responses can lead to higher cytokine concentrations in plasma, as observed in patients with IFN-γ or GM-CSF receptor deficiencies[79–81]. We hypothesized that impaired cytokine responses due to low JAK2 levels might increase cytokine concentrations in the plasma of MCTS1-deficient patients. We assessed the levels

Author Manuscript Author Manuscript Author Manuscript Author Manuscript

of 13 JAK2-dependent cytokines (Table S6) by bead-based ELISA. We found no detectable increase in plasma cytokine levels in the patients tested (Figure S7R). Finally, as another control, we tested the response to another JAK2-mediated cytokine, IL-27, in the patients' T-cell blasts. We found a normal response to several concentrations of IL-27, in terms of STAT1 and STAT3 phosphorylation in T-cell blasts from patients, relative to healthy controls (Figure S7S,T). Thus, the biological response to IL-23 is tightly dependent on JAK2 levels, to a greater extent than responses to other JAK2-dependent cytokines, including IL-12, IL-27, and IFN-γ. These findings are consistent with the clinical phenotype of MCTS1-deficient patients being restricted to MSMD (Table S6).

## Defective IL-23 response pathway in the PBMCs of patients with MCTS1 deficiency

Having shown that responses to IL-23 were impaired in the patients' T-cell blasts, we investigated the responses of peripheral blood mononuclear cells (PBMCs) from the patients. We stimulated fresh PBMCs with IL-12, IL-23, or phorbol 12-myristate 13-acetate (PMA) plus ionomycin for 48 hours and measured IFN-γ levels in the medium. We found that levels of IFN-γ production by PBMCs from MCTS1-deficient patients were 10-fold lower after IL-12 treatment and 23-fold lower after IL-23 treatment than those of controls (Figure 6A), whereas IFN-γ production was normal after stimulation with PMA plus ionomycin. No *IFNG* mRNA induction upon IL-23 stimulation was observed in the PBMCs of MCTS1-deficient patients, whereas a 33-fold induction was observed in controls (Figure 6B), suggesting that this defect was not due to an impairment of *IFNG* mRNA translation. We also observed that the amounts of TNF produced in response to IL-23 stimulation were 23-fold lower in cells from patients than in those of controls (Figure S7U). For these samples, RNA sequencing revealed a significant induction of 291 genes upon stimulation with IL-23 in healthy controls, but no significant induction of any gene in MCTS-deficient patients (Table S8). An analysis of the correlation of the changes in expression of these 291 genes revealed a broadly impaired response to IL-23 in the PBMCs of MCTS1-deficient patients (Figure 6C). Modular repertoire analysis revealed that genes related to innate inflammation (inflammation, cytokines, monocytes, neutrophils), plasma cells, interferon and oxidative stress were poorly induced in the patients' cells (Figure 6D), probably due to the combined low levels of stimulation of the IL-23 and IFN-γ response pathways, the latter being due to impaired IFN-γ production. Control cryopreserved PBMCs produced no detectable IFN-γ upon IL-23 stimulation (Figure 6E, condition 2) and required co-stimulation with IL-1ß to produce detectable amounts of IFN-γ upon IL-23 stimulation (Figure 6E, condition 4)[35]. Assessments of the response to IL-23 in the presence of IL-1ß also revealed a defect in cryopreserved PBMCs from MCTS1-deficient patients (Figure 6E, condition 3 versus condition 4). Cellular responses to IL-12 and IL-12 plus IL-1β were also partially impaired in the patients (Figure 6E, conditions 5 and 6). MCTS1-deficient PBMCs, thus, phenocopied PBMCs with *TYK2* mutations (*TYK2*$^{-/-}$ and *TYK2* P1104A/P1104A) (Figure 6E). The patients' PBMCs responded poorly to IL-23, with such stimulation failing, in particular, to induce IFN-γ.

## Impaired IFNG mRNA induction by IL-23 in Vδ2$^{+}$ γδ T, MAIT and $T_H1$* cells

IFN-γ is mostly produced by T and NK lymphocytes[84]. Upon IL-23 stimulation, innate NK cells and innate-like adaptive Vδ2$^{+}$ γδ T and MAIT cells are particularly potent

Author Manuscript Author Manuscript Author Manuscript Author Manuscript

producers of IFN-γ[30,42]. We hypothesized that some of these lymphocyte subsets might display impaired IFN-γ production in response to IL-23 stimulation in MCTS1-deficient patients. We tested this hypothesis, by stimulating cryopreserved PBMCs from seven healthy controls, four MCTS1-deficient patients, two IL-23R-deficient patients and one IL-12Rβ1-deficient patient with IL-23 for six hours and then performing single-cell RNA sequencing (scRNA-seq). This dataset incorporates several samples previously studied by Ogishi et al.[35] and Philippot et al.[42]. After batch correction with Harmony and graph-based unsupervised clustering (Figure S8A–C), we were able to identify most PBMC leukocyte subsets (Figure 7A, Figure S8D–E). As previously reported, NK, Vδ2$^+$ γδ T, and MAIT cells were the major subsets displaying *IFNG* induction upon IL-23 stimulation (Figure S8F). As reported for patients with IL-23R or IL-12ßR1 deficiency, MCTS1-deficient Vδ2$^+$ γδ T and MAIT cells displayed impaired *IFNG* induction following IL-23 stimulation relative to healthy controls (Figure 7B, Figure S8G). The induction of *IFNG* expression was also impaired in purely adaptive Th1* cells, which normally produce less IFN-γ in response to IL-23 than innate-like T cells[42]. By contrast to IL-23R and IL-12Rβ1 deficiencies, the induction of *IFNG* by NK cells was moderately impaired in MCTS1-deficient patients (Figure 7B, Figure S8G). We also observed a broadly impaired transcriptional response to IL-23 stimulation in MCTS1-deficient PBMCs, resembling that seen in IL-12Rβ1- and IL-23R-deficient PBMCs (Figure 7C). This global transcriptional response probably represents a combination of the cellular responses to IL-23 and to the IFN-γ secreted in response to IL-23, as observed for example in monocytes following the stimulation of MCTS1-deficient PBMCs with IL-23 (Figure 7D). Overall, the response to IL-23 is impaired in the Vδ2$^+$ γδ T, MAIT, and $T_H1$* cells of MCTS1-deficient patients, leading to an impairment of *IFNG* mRNA induction by these cells in response to stimulation with IL-23.

## Impaired induction of IFN-γ secretion by IL-23 in Vδ2$^+$ γδ T and MAIT cells

We then investigated the possibility that the impaired response to IL-23 in Vδ2$^+$ γδ T and MAIT cells might impair the response of these cells to mycobacterial infection. We treated cryopreserved PBMCs with various stimuli, including the two cytokines (IL-12, IL-23), BCG, alone or with either or both cytokines, for 48 hours and assessed the amount of IFN-γ generated by these lymphocyte subsets by intracellular staining and flow cytometry. Consistent with our previous results, we found that IFN-γ production by Vδ2$^+$ γδ T and MAIT cells upon stimulation with IL-23, BCG, or IL-23 plus BCG, was defective relative to that in healthy controls (Figure 7E–F). Interestingly, IFN-γ production was impaired only very mildly, if at all, in NK cells (Figure 7G). We investigated whether Vδ2$^+$ γδ T and MAIT cells had a stronger defect of JAK2 expression than other T cells. We generated T-cell blasts from sorted CD4$^+$, Vδ2$^+$ γδ T, or MAIT cells (Figure S8H) and measured their JAK2 levels by western blotting. All T-cell blasts had low levels of JAK2 (Figure S8I), but the defect was not stronger in Vδ2$^+$ γδ T-cell and MAIT blasts. Nevertheless, P2's primary T-cell blasts displayed a stronger mean decrease in JAK2 expression than the primary myeloid cells of P2 (particularly MDMs and MOCs) (Figure S8J). This suggests that the specific impairment of the IL-23 response pathway and the partial impairment of the IL-12 response pathway in MCTS1-deficient patients could be explained in part by stronger JAK2 depletion in T lymphocytes than in myeloid cells. In summary, JAK2 expression

Author Manuscript Author Manuscript Author Manuscript Author Manuscript

and IL-23-dependent IFN-γ production are impaired in the Vδ2$^+$ γδ T and MAIT cells of MCTS1-deficient patients.

## Discussion

We describe a surprising, new genetic etiology of MSMD: XR MCTS1 deficiency in six male individuals from five unrelated kindreds and four distant ancestries. Complete MCTS1 deficiency impairs ribosome recycling and translation reinitiation in the patients' cells. JAK2 is one of about 150 human genes subject to MCTS1-mediated translation re-initiation. JAK2 protein levels in MCTS1-deficient myeloid and lymphoid cells are about three- to four-fold lower than those in control cells, with a greater decrease in levels observed in lymphoid than in myeloid cells. Responses to IFN-γ and IL-12, both of which normally require JAK2, were normal in these cells. By contrast, the response to IL-23 was impaired in the patients' T-cell blasts and MCTS1 KO HEK Blue cells, which was rescued by exogenous expression of MCTS1 or JAK2. The patients MAIT and Vδ2$^+$ γδ T-lymphocyte subsets produce only small amounts of IFN-γ in response to IL-23 and BCG. We show here that decreases in JAK2 levels or activity impair IL-23-dependent IFN-γ production by lymphocytes, providing a molecular and cellular basis for disease, and mechanistically and causally connecting the *MCTS1* genotype and the MSMD phenotype. Remarkably, an unbiased genome-wide forward genetics approach revealed an unexpected MSMD phenotype in patients with human MCTS1 deficiency.

Our finding is unexpected because MCTS1 is ubiquitously expressed and has a fundamental molecular function in the dissociation of deacylated tRNAs from post-termination 40S ribosomal complexes during ribosome recycling (on mORF stop codons) and re-initiation (on uORF stop codons). The translation re-initiation functions of DENR and MCTS1 are essentially identical in amplitude [58,59,62]. However, DENR$^{KO}$ is embryonically lethal in mice, whereas MCTS1$^{KO}$ mice are viable [60]. This is consistent with the more severe ribosome recycling defect of DENR$^{KO}$ HeLa cells than of MCTS1$^{KO}$ HeLa cells. Furthermore, we found no MSMD patient homozygous for rare candidate DENR variants. The apparent lack or extreme rarity of DENR-deficient patients suggests that this deficiency may be embryonically lethal in humans, as it is in mice. This contrasts with our findings that all five patients with MCTS1 deficiency have isolated MSMD and are otherwise healthy at ages of six months to 18 years. However, only one MCTS1-deficient patient has yet reached adulthood, and other clinical phenotypes may appear as the patients age.

We define the set of human MCTS1-dependent genes in cells from MCTS1-deficient patients. We identify JAK2 as a translational target of DENR-MCTS1 and probably the key contributor to MSMD. Decreases in the levels of other MCTS1-dependent proteins do not appear to have clinical consequences. Surprisingly, partial JAK2 deficiency impairs cellular responses to IL-23 and the subsequent induction of IFN-γ in lymphocytes, but not other cytokine response pathways involving JAK2. DENR$^{KO}$ has been reported to impair JAK2 translation and subsequent responses to IFN-γ in mouse tumor cells[85]. Responses to IL-12 and IL-23 were not tested in this previous study. We found the same connection between MCTS1 and JAK2 in human cells, but the response to IFN-γ was intact. Low levels of JAK2 may have a much greater effect in IL-23- and IL-12-responsive cells than in IFN-γ-

Author Manuscript Author Manuscript Author Manuscript Author Manuscript

responsive cells. It is probably no coincidence that the four types of MSMD-causing *TYK2* variants, including the common P1104A variant, have an impact on the IL-23 response pathway, whereas only two of these types of variants also impair responses to IL-12[35]. This finding suggests that the IL-23R is more dependent on qualitative and quantitative variations of JAK2 or TYK2 than the IL-12R. Biochemical differences may be responsible for the weaker IL-23R signaling observed.

Our findings support our previous reports that human IL-23 is a key IFN-γ-inducing cytokine[18,30,42,73]. Despite having the p40 chain in common, IL-23 has historically been seen as an IL-17-inducing cytokine[73,88–91], whereas IL-12 is seen as the key IFN-γ-inducing cytokine[73,91]. Recent discoveries have suggested that human IL-23 plays a key role in IFN-γ-mediated immunity to mycobacteria, and a more minor role in IL-17-mediated immunity to fungi. First, AR complete IL-23R deficiency underlies MSMD with almost complete clinical penetrance but only a mild form of CMC with incomplete penetrance[30,42]. Second, homozygosity for the common TYK2 P1104A allele selectively impairs responses to IL-23 and underlies MSMD with low penetrance and tuberculosis with high penetrance, but has no effect on susceptibility to CMC[18,54]. Third, impairment of the cellular response to IL-23 is the only mechanism underlying mycobacterial disease common to patients with the five forms of AR TYK2 deficiency[28,60]. Fourth, MCTS1-deficient patients have impaired cellular responses to IL-23 and isolated MSMD, with no detectable IL-17 deficiency or CMC. Collectively, these observations suggest that human IL-23 acts more as an IFNγ-inducing antimycobacterial cytokine than as an IL-17-inducing antifungal cytokine.

We found that IFN-γ induction in response to IL-23 stimulation was impaired in the Vδ2$^+$ γδ T and MAIT cells of MCTS1-deficient patients. This finding is consistent with previous reports, as Vδ2$^+$ γδ T and MAIT cells are among the subsets producing the largest amounts of IFN-γ in response to IL-23[30,42]. Furthermore, the IFN-γ production of these cells in response to IL-23 is impaired in IL-12Rβ1$^{-/-}$, IL-23R$^{-/-}$ and TYK2$^{-/-}$ individuals[30,42,60]. NK cells are also potent inducers of IFN-γ upon stimulation with IL-23, but their transcriptional response to IL-23 is only moderately impaired in MCTS1-deficient patients. Interestingly, the induction of IFN-γ was also impaired in the patients' TH1* cells. TH1* cells have a lower level of IFN-γ induction than MAIT, Vδ2$^+$ γδ T and NK cells. Nonetheless, TH1* cells display more than an eight-fold induction of IFN-γ in response to IL-23 (Figure S8F), this induction being totally abolished in MCTS1-, IL-12Rβ1-, and IL-23R-deficient patients. TH1* cells are the major lymphocyte subset producing IFN-γ after exposure to BCG *in vitro*[92,93]. The counts of these cells in the blood increase in individuals with latent tuberculosis infection[94]. IL-23 may, thus, also contribute to TH1*-mediated immunity to mycobacteria.

Finally, we can speculate about the clinical phenotype of MCTS1-deficient patients in the absence of BCG vaccination. Surprisingly, none of the six MCTS1-deficient individuals had EM disease. This may be due to the protection afforded by BCG disease, as seen in IL-12Rß1-deficient patients[38,39]. It may also reflect an incomplete IFN-γ deficit, as only one of the seven reported IL-23R-deficient patients suffered from EM disease[41,42] and cellular responses to IL-23 are impaired, but not abolished in MCTS1-deficient patients. In regions of endemic tuberculosis, in which BCG vaccination is not widely or efficiently

Author Manuscript Author Manuscript Author Manuscript Author Manuscript

performed, or if penetrance for BCG disease is incomplete, MCTS1 deficiency may be revealed by severe tuberculosis. Overall, this study reveals a surprising mechanistic connection between deficiency of a basic, ubiquitous, biochemical mechanism and a selective predisposition to mycobacterial disease.

### Limitations of the study

The five unrelated patients studied are all relatively young, between 1 and 18 years of age. We cannot therefore rule out the possibility of hitherto undetected clinical phenotypes other than MSMD arising as the patients age. We demonstrated that there is an impaired response to IL-23 in MCTS1$^{KO}$ HEK-Blue cells and that this can be rescued by JAK2 overexpression. This suggests that the impaired IL-23 response in MCTS1 deficient patients is solely due to reduced levels of JAK2 expression. Yet, we have not, for technical limitations, carried out this rescue experiment in PBMCs of the patients and can therefore not completely rule out the possibility that other MCTS1 targets contribute to the phenotype *in vivo*.

## STAR METHODS

### RESOURCE AVAILABILITY

**Lead contact—**Further information and requests for resources and reagents should be directed to and will be fulfilled by the lead contact, Jonathan Bohlen (jonathan.bohlen@institutimagine.org).

**Materials availability—**All raw and processed data and biological materials, including immortalized cell lines from patients, are available upon request from the lead contact under a Material/Data Transfer Agreement with Inserm or the Rockefeller University.

**Data and Code Availability—**The RNA-seq, single-cell RNA-seq, and CITE-seq data have been deposited at SRA and are available at project ID PRJNA1004232. Custom software is available from GitHub: https://github.com/aureliioteleman/Teleman-Lab. The original western-blot images, flow cytometry data, mass spectrometry data, and microscopy data reported in this paper will be shared by the lead contact upon request.

Any additional information required to reanalyze the data reported in this paper can be obtained from the lead contact upon request.

This paper does not report original code.

### EXPERIMENTAL MODEL AND STUDY PARTICIPANT DETAILS

The age, sex, ancestry and race of the studied patients is reported in the main text of the paper and in the method details below. Information on gender and socioeconomic status of the patients was not collected. All patients are male because we study an X-linked recessive genetic disease. Informed consent was obtained in the countries of residence of the patients, in accordance with local regulations (kindred A in China, kindred B in Finland, kindred C in Saudi Arabia and kindreds D and E in Iran) and with institutional review board (IRB) approval. Experiments were conducted in France, Germany, Qatar, and the United States of America, in accordance with local regulations and with the approval of the IRB

Author Manuscript Author Manuscript Author Manuscript Author Manuscript

of the Rockefeller University (protocol no. JCA-0699) and INSERM (protocol no. C10-07 and C10-16) and by the Institutional Research Ethics Boards of Sidra Medicine and Qatar Biobank, for the United States of America, France and Qatar, respectively. Healthy controls were recruited in Finland, France, Iran, Saudi Arabia, and the United States of America.

## METHODS DETAILS

**Human patients—**Informed consent was obtained in the countries of residence of the patients, in accordance with local regulations (kindred A in China, kindred B in Finland, kindred C in Saudi Arabia and kindreds D and E in Iran) and with institutional review board (IRB) approval. A detailed questionnaire was completed by the physicians caring for the patients, including demographic data, clinical features, and biological and microbiological results, and the data were sent to J.Bo., Q.Zha. and J.Bu. A detailed clinical case report is provided below.

### Case reports

**Kindred A, P1.:** P1 was the third child of nonconsanguineous parents of Chinese origin, with two healthy older sisters (Table S1, Figure 1A). He was born at full term in 2017, with no perinatal complications. He received the BCG vaccine (Danish strain) on the day after delivery. He was well until seven months of age, when an enlarged left axillary lymph node that was erythematous and tender was detected. Surgical incision and drainage were performed, but the local lesions relapsed. The lymph node under the mandibular region was also found to be enlarged. At the age of 14 months, P1 had recurrent fever associated with hepatosplenomegaly, chest wall abscess and osteomyelitis with multiple bone lesions. A computerized tomography (CT) scan showed an enlarged lymph node under the left armpit, with necrosis, multiple sublobe atelectasis in the left lung, multiple abscesses in the spleen, lesions in the ribs on both sides of the body, multiple vertebrae, and the right ilium. Hepatosplenomegaly was confirmed by CT-scan. Acid-fast bacilli (AFB) were detected in the abscess and disseminated mycobacterial infection (BCG-osis) was diagnosed. The whole metagenome of the abscess was shotgun-sequenced, and *Mycobacterium bovis* BCG was detected. Antimycobacterial treatment was implemented, based on isoniazid (INH), rifampin (RIF), ethambutol (EMB), amikacin, and linezolid; subcutaneous treatment with recombinant IFN-γ was also initiated. However, the patient's medical condition deteriorated, and the patient died in 2019.

**Kindred B, P2.:** P2 is a boy originating from and living in Finland (Table S1, Figure 1A). He was born in 2003 and received the BCG vaccine (Danish strain) at birth. Three months later, he developed BCG-itis consisting of an enlarged lymph node in the left groin. On ultrasound examination, intra-abdominal lymph nodes were detected, with para-iliac and para-aortic extension. One lymph node was excised and cultured, yielding *M. bovis* BCG. P2 progressively developed a high fever, tiredness and poor appetite, and a diagnosis of disseminated BCG-osis was established. Treatment with INH, RIF, EMB, ciprofloxacin, amikacin and IFN-γ was initiated and the patient recovered well. Treatment with four antimycobacterial drugs (excluding amikacin) and IFN-γ was continued for one year, and drug treatment was then gradually stopped. When P2 was two years and nine months old and on RIF/INH, the symptoms recurred, a severe relapse was diagnosed and treatment with five

Author Manuscript Author Manuscript Author Manuscript Author Manuscript

drugs plus IFN-γ was reinstated. At the age of five years, P2 was well, with no symptoms, a normal chest X ray and abdominal ultrasound results, and was treated with RIF/INH/IFN-γ twice weekly. At his most recent consultations (in 2019 and 2021), he was well, without treatment. No other severe infections have occurred. P2 has a healthy sister who is growing normally. P2 received all other routinely indicated vaccines without complication. At five years of age, he was assessed by a neurologist for learning difficulties, but no neurological issues were identified and magnetic resonance imaging (MRI) was not indicated. At the age of seven years, a CT scan of the head, thorax and upper abdomen showed no abnormalities. Abdominal ultrasound was performed yearly until the age of nine years, and all the organs detected were of normal size and development. At the age of 16 years, the patient consulted an endocrinologist as he was slightly overweight. Thyrotropin-releasing hormone (TRH) stimulation test results and the levels of sex hormones, T3 and TSH were all normal. T4V levels were slightly below the lower limit of the normal range. The patient was therefore considered healthy. He swims, skis, and rides horses and motorbikes.

**Kindred C, P3.:** P3 is a boy originating from and living in Saudi Arabia (Table S1, Figure 1A). He was born in 2010 and received the BCG vaccine (Danish strain) at birth. At the age of one year, he underwent excision of the left axillary lymph node due to BCG-itis. At the age of three years, he was referred to the hospital for painful swelling of the distal third of the left leg of six months' duration. An X ray of the left leg showed an intramedullary lytic lesion with surrounding cortical thickening at the diaphysis of the distal tibia, and magnetic resonance imaging (MRI) results were suggestive of chronic osteomyelitis, with a lesion in the distal tibia diaphysis measuring 5.2 cm x 1.1 cm associated with an extensive periosteal reaction. A biopsy was performed on the left tibia; histological examination revealed inflammatory granulation, and *M. bovis* BCG susceptible to INH, RIF, and EMB and resistant to pyrazinamide (PZA) grew in culture. P3 was treated with INH, RIF, and clarithromycin for 12 months, with an excellent clinical response resulting in total resolution. Immunophenotyping results for T, B and NK cells, immunoglobulin levels (IgG, IgM and IgA) and oxidative burst assay (in neutrophils) results were normal. The patient is currently 12 years old, alive and well, and performing well at school. He presented no unusual infections during follow-up and was fully immunized according to the usual schedule, with no adverse effects. P3 has four sisters and one brother, who is 18 years old and healthy, and, like the sisters, presented no complications after BCG vaccination or severe/atypical infections.

**Kindred D, P4.:** P4 is a boy, born in 2016 to nonconsanguineous parents from Iran (Table S1, Figure 1A). He received the BCG vaccine (Pasteur 1173p2 strain) at birth. He was hospitalized at the age of five months for right axillary lymphadenopathy. He developed an abscess with pus discharge in this area. An ultrasound scan of the axillary area revealed an internal echogenic mass (4.2 x 3.4 x 2.7 cm) and another hypoechoic node (3.7 x 3.3 x 1.5 cm). PCR results were positive for *M. tuberculosis* complex and culture confirmed *M. bovis* BCG infection. P4 received INH, EMB, RIF and levofloxacin supplemented with folic acid and vitamins, but the parents stopped the treatment after four months. Nine months later, P4 suffered another right axillary lymphadenopathy with pus discharge and fever. PCR was positive for *M. tuberculosis* complex. The patient received treatment with INH,

Author Manuscript Author Manuscript Author Manuscript Author Manuscript

EMB and clarithromycin for nine months. Abdominal ultrasound results and a bone scan were normal. P4 presented no infection with any other organism and was in good health, except for his low Ig levels. He is currently in good health, on monthly IVIG treatment for his low Ig levels. He has no siblings, and there is no history of IEI in his relatives and cousins. His mother had a history of abortion due to the absence of a fetal heartbeat and a neural tube defect at 16 weeks of pregnancy. At the age of five months, P4 underwent abdominal ultrasound and abdominopelvic CT scans. All the organs detected were of normal size and development. P4 is now seven years old. He is physically active, plays football and socializes with his peers. His growth is normal, and abdominal and pelvic ultrasound scans show the detected organs (including the liver, spleen, bile ducts, gallbladder, pancreas, kidneys and urinary bladder) to be normal in size and development.

**Kindred E, P5, P6 and P7.:** P5 was born to consanguineous Iranian parents in 2019 (Table S1, Figure 1A). He was vaccinated with BCG (Pasteur 1173P2 strain) at birth. At the age of three months, he presented a left axillary draining adenopathy, which was resected surgically at seven months. Histological analysis of the lymph node showed an epithelioid granuloma containing AFB. The presence of BCG was documented by PCR. P5 was treated with RIF and INH for six months. At 13 months of age, he developed ascites, multiple abdominal adenopathies, and hepatic calcified nodules. Ascitic fluid analysis revealed a lymphocytic exudate. Liver biopsy showed cirrhosis, but no mycobacterial elements were documented. Bone marrow biopsy results were normal. P5 received antimycobacterial treatment with RIF, INH, EMB, ofloxacin and clarithromycin for nine months. He is currently well without treatment, with mild hepatosplenomegaly but no other symptoms. P5 has a sister who is well and has never been hospitalized, and a brother (**P7**) who was identified as a mutation carrier a few days after birth and was therefore not vaccinated with BCG; P7 has no history of mycobacterial infection. The height and weight of P5 and P7 have been routinely monitored and no abnormalities have been found. P5 and P7 also had an uncle (**P6**), the brother of their mother, who died at the age of two years from fever and hepatosplenomegaly. P6 was vaccinated with BCG (Pasteur 1173P2 strain) at birth.

**WES and Sanger sequencing—**For P1, genomic DNA (gDNA) was extracted with the Qiagen blood mini kit, and DNA fragments were generated and enriched for whole-exome sequencing with the Agilent SureSelect XT Human All Exon V5 kit. Sequencing was performed on an Illumina HiSeq X10 apparatus (Illumina). Reads were mapped on the human reference genome [95] with Burrows-Wheeler aligner-0.7.12 [96]. Variant calling was then performed on the aligned reads, with GATK-3.4-46 best practices [97]. For annotation of the variants, we used SnpEff-4.1a [98] tools. For P2, P3 and P4, gDNA was isolated from whole blood with the iPrep PureLink gDNA Blood Kit and iPrep Instruments (Life Technologies, Thermo Fisher Scientific). Exome capture was performed with the SureSelect Human All Exon 50 Mb kit (Agilent Technologies), with 3 μg gDNA. Single-end sequencing was performed on an Illumina Genome Analyzer IIx (Illumina). For P5, gDNA was isolated from whole blood. WES was performed at Macrogen Korea (Macrogen, Inc., Seoul, South Korea). For WES, exon enrichment was performed with the SureSelect XT Library Prep Kit (Agilent Technologies, CA, USA). Sequencing was performed on a NovaSeq 6000 (Illumina, CA, USA) sequencer generating 150 bp reads, with 100×

Author Manuscript Author Manuscript Author Manuscript Author Manuscript

coverage. The NGS platform generally covered >95% of the targeted regions with up to 99% sensitivity.

All variants from the patients and their familial segregation (when appropriate materials were available for analysis) were confirmed by amplifying the flanking regions of the variants obtained with specific primers (Figure S1A–E). PCR products were analyzed by electrophoresis in 1% agarose gels, sequenced with the Big Dye Terminator v3.1 cycle sequencing kit (Applied Biosystems), and analyzed on an ABI Prism 3700 sequencer (Applied Biosystems).

**Enrichment analysis—**We performed an enrichment analysis for pLOF variants of the *MCTS1* gene on our cohort of 422 male patients with MSMD of unidentified genetic etiology. As controls, we used 1,932 male individuals of diverse ethnic origins from our in-house database. These controls were patients with various genetically unexplained non-mycobacterial infections other than chronic mucocutaneous candidiasis (CMC). We used the Firth penalized logistic regression method [99], as implemented in the R (v4.1) [100] package logistf, to compare the proportion of individuals with pLOF variants between the MSMD and control groups. The analysis was adjusted for the first five principal components (PCs) to account for the ethnic heterogeneity of the samples. Principal component analysis (PCA) was performed with Plink v1.9 software on WES data, with the 1000 Genomes (1kG) Project phase 3 public database as a reference, for 2,942 exonic variants with minor allele frequency (MAF) > 1% and a call rate > 99%.

**Exon trapping assay—**A DNA segment encompassing the *MCTS1* exon 2 and 3 region (ChrX: 120604950 to ChrX: 120606870 region, GRCh38 reference, release 13) was amplified from genomic DNA extracted from whole-blood samples from a healthy control. It was inserted between the *Xho*I and *Bam*HI sites of the pSPL3 vector. The sequence was then mutated to encode the variant of P3. Plasmids containing wild-type (WT) and mutant *MCTS1* exon 2-3 regions were then used to transfect COS-7 cells. After 24 hours, total RNA was extracted and reverse-transcribed. The cDNA products were amplified with primers binding to the flanking HIV-TAT sequences of the pSPL3 vector and ligated into the pCR™4-TOPO® vector (Invitrogen). Stellar™ cells (Takara) were transformed with the resulting plasmids. Colony PCR and sequencing with primers binding to the flanking HIV-TAT sequences of pSPL3 were performed to assess the splicing products transcribed from the WT and mutant alleles.

**Patient-derived cell lines—***Herpesvirus saimiri*-transformed T (HVS-T) cells were generated with the TERT transformation system. HVS-T cells were cultured in 40% RPMI, 40% Panserin 401, 20% fetal-calf serum (FCS) supplemented with 10 ng/ml IL-2, 50 μg/ml gentamycin (Gibco, 15750060) and GlutaMAX™ (Gibco, 35050061). T-cell blasts (T-blasts) were induced from 2 million PBMCs (fresh or cryopreserved) in 2 ml ImmunoCult™-XF T Cell Expansion Medium (Stem Cell Technologies, 10981) supplemented with 10 ng/ml IL-2 (Gibco, PHC0023) and 1:40 diluted ImmunoCult™ Human CD3/CD28/CD2 T Cell Activator. T-blasts were then cultured in ImmunoCult medium with IL-2 for 2-3 weeks, before restimulation in the same manner. Dermal primary fibroblasts were obtained from

Author Manuscript Author Manuscript Author Manuscript Author Manuscript

skin biopsy specimens, transformed with SV40 antigen and cultured in DMEM (Gibco) supplemented with 10% FCS. All cell lines used tested negative for mycoplasma.

**Cell-line culture—**We cultured HeLa cells, HEK293T cells, γ2A- fibrosarcoma cells and HT1080 cells in DMEM +10% FCS +100 U/ml penicillin/streptomycin (Gibco 15140122). We subcultured the cells with trypsin-EDTA. HeLa cells tested negative for mycoplasma and were authenticated by SNP typing. THP-1 cells were cultured in RPMI supplemented with 10% FCS.

**Translation reporter assays—**HeLa cells were used to seed 96-well plates at a density of 8,000 cells per well. Cells were transfected for 16-20 hours in the presence of Lipofectamine 2000, with 100 ng *Renilla* luciferase plasmid and 100 ng firefly luciferase plasmid per well. For translation reporter assays including MCTS1 reconstitution conditions, we used 60 ng of EV, *MCTS1* WT or variant expression plasmid, 70 ng of *Renilla* luciferase reporter plasmid and 70 ng of firefly reporter plasmid per well. Four hours after transfection, the medium was replaced. All the *Renilla* luciferase plasmids contained the 5'UTR of interest, whereas all the firefly luciferase plasmids contained the MCTS1-independent *Lamin B1* 5'UTR and were used as a transfection normalization control. We added 0.4 μl Lipofectamine reagent to each well. Cell transfection was always performed with technical triplicates. Luciferase activity was assessed 16-20 hours after transfection, with the Promega Dual-Luciferase® Reporter Assay System, in accordance with the manufacturer's instructions.

**40S and 80S ribosome footprinting—**We performed 40S and 80S ribosome footprinting, as previously described [65,101]. Briefly, HeLa cells and SV40-fibroblasts were grown to ~80% confluence in multiple 15 cm dishes (2-3 dishes per treatment). The cells were briefly washed with 1x PBS, 10 mM $MgCl_2$, and 400 μM cycloheximide, and freshly prepared crosslinking solution (1x PBS, 10 mM $MgCl_2$, 400 μM cycloheximide, 0.025% PFA, 0.5 mM DSP) was added. Cells were incubated with crosslinking solution for 15 minutes at room temperature with slow rocking. The crosslinking solution was then poured off and the remaining crosslinker was inactivated by incubation for 5 minutes with ice-cold quenching solution (1x PBS, 10 mM $MgCl_2$, 200 μM cycloheximide, 300 mM glycine). The quenching solution was poured off and 150 μl lysis buffer (0.25 M HEPES pH 7.5, 50 mM $MgCl_2$, 1 M KCl, 5% NP40, 1000 μM cycloheximide) was added to each 15 cm dish. The cells were incubated at 4°C for two minutes for lysis. The cell debris was scraped off the dish and the lysate was collected. The lysates were briefly vortexed and clarified by centrifugation at 20,000 x *g* for 10 minutes at 4°C. The supernatant was collected and its RNA concentration was determined with a Nanodrop spectrophotometer. We then added 100 U RNAse 1 (Ambion, AM2294) per 120 μg of RNA. Lysates were incubated for 5 minutes at 4°C and then loaded onto 17.5%-50% sucrose gradients and centrifuged for 5 hours at 35,000 rpm in a Beckman Ultracentrifuge equipped with an SW40 rotor. Gradients were fractionated with a Biocomp Gradient Profiler system. We collected the 40S and 80S fractions for immunoprecipitation and footprint isolation. The 40S and 80S fractions corresponding to one or two 15 cm dishes were used for the direct extraction of RNA for total footprint samples. The crosslinker was then removed and RNA was extracted

Author Manuscript Author Manuscript Author Manuscript Author Manuscript

from the footprint fractions: 55 µl (1/9 volume) of crosslink-removal solution (10% SDS, 100 mM EDTA, 50 mM DTT) and 600 µl acid-phenol chloroform (Ambion) were added and the mixture was incubated at 65°C, with shaking at 1,300 rpm for 45 minutes. The tubes were then placed on ice for 5 minutes and centrifuged for 5 minutes at 20,000 x *g*. The supernatant was washed once with acid-phenol chloroform and twice with chloroform, and the RNA was then precipitated with isopropanol and used for library preparation (see below). The precipitated or total proteins were isolated from the organic phase. We added 300 µl ethanol and 1.5 ml isopropanol and the solutions were incubated at −20°C for 1 hour. Proteins were sedimented by centrifugation at 20,000 x *g* for 20 minutes, washed twice with 95% ethanol and 0.3 M guanidine-HCl, dried and resuspended in 1x Laemmli buffer.

**Deep-sequencing library preparation—**The quality and integrity of the 40S and 80S RNA extracted were determined on an Agilent Bioanalyzer with the total RNA Nano 6000 Chip. For size selection, RNA was subjected to electrophoresis in 15% urea-polyacrylamide gels (Invitrogen) and fragments of 20-80 nt (40S) or 25-35 nt (80S) in size were excised, with the Agilent small RNA ladder used as a reference. RNA was extracted from the gel pieces by smashing the gels into small pieces with gel smasher tubes and extracting the RNA in 0.5 ml 10 mM Tris pH 7 at 70°C for 10 minutes. The gel pieces were removed and RNA was precipitated in isopropanol. The RNA was then dephosphorylated by incubation with T4 PNK (NEB, M0201S) for 2 hours at 37°C in PNK buffer without ATP. It was precipitated again and purified in isopropanol. Footprints were then analyzed with an Agilent Bioanalyzer small-RNA chip and the Qubit smRNA kit. We used up to 25 ng of footprint RNA as input for library preparation with the SMARTer smRNA-SeqKit for Illumina from Takara/Clontech Laboratories, according to the manufacturer's instructions. For RNA-seq libraries, total cell RNA was extracted with TRIzol and libraries were prepared with the Illumina TruSeq stranded library preparation kit. Deep-sequencing libraries were sequenced on the Illumina Next-Seq 550 system.

**Data analysis and statistics—**Analysis of ribosome footprinting NGS data: Adapter poly-A sequence nucleotides were trimmed from raw reads with cutadapt (https://doi.org/10.14806/ej.17.1.200). Ribosomal RNA and tRNA reads were removed by bowtie2 alignment with human tRNA and rRNA sequences [102]. The remaining reads were then separately aligned with the human transcriptome (Ensembl transcript assembly 94) and the human genome (hg38) with BBmap (sourceforge.net/projects/bbmap/). Counted reads were generally normalized by sequencing depth (number of alignments per library). Reads were counted, and metagene plots and single-transcript traces were obtained with custom software written in C and available from GitHub (https://github.com/aureliioteleman/Teleman-Lab). Translation efficiency (TE) was calculated from the number of 80S ribosome footprints in a coding sequence divided by the number of RNA sequencing reads on the coding sequence. uORFs were annotated on the basis of the presence of an ATG and an inframe stop codon within the 5'UTR of any mRNA. Only uORFs beginning with an ATG were considered.

**Stable lentiviral transduction—**Lentiviral particles were produced in HEK293T cells by transfection with pPAX2, pHBX2, pVSV-G and pTRIP EV or plasmids containing the *MCTS1* variants, with X-tremeGENE 9 (Roche, 6365779001). The medium was

Author Manuscript Author Manuscript Author Manuscript Author Manuscript

replaced after five hours. The supernatant was harvested 20 hours post-transfection, filtered, supplemented with 8 μg/ml protamine sulfate and added, in a 1:1 volumetric ratio, to 150,000 cells in 100 μl medium. Cells were spinoculated for 2 hours at 1200 x *g*. The cells were cultured for three to four days, assayed for transgene expression by FACS staining for ΔNGFR, and subjected to enrichment for MACS sorting.

**Generation of MCTS1 and JAK2 knockouts in THP-1 cells and HEK-Blue IL-23 cells—**THP-1 cells or HEK-Blue IL-23 cells were transduced with pLENTI-V2 constructs encoding Cas9 and an sgRNA (GCCTGGGAAGGATACAACAA) targeting the *MCTS1* gene and an sgRNA targeting *JAK2* (GGTAAGAATGTCTTGTAGCT). Cells were then selected by culture with 5 μg/ml (THP-1) or 1 μg/ml (HEK-Blue) puromycin for two weeks. The KO pool was then tested for efficient knockout by western blotting, and seeding was performed by limiting dilution for clonal expansion. Clones were screened by western blotting and *MCTS1* knockout was confirmed by gDNA sequencing.

**Immunoblotting—**Cells were lysed in standard RIPA lysis buffer containing protease inhibitors (Roche mini EDTA-free, 1 tablet in 10 ml) and phosphatase inhibitors (2 mM sodium Ortho-vanadate, Roche Phosstop 1 tablet in 10 ml, 0.1 M sodium fluoride, 0.1 M beta-glycerophosphate) and Benzonase (50 U/ml), after brief washing in FCS-free DMEM or PBS. Lysates were clarified and protein concentration was determined in a BCA or Bradford assay. Equal amounts of protein were subjected to SDS-PAGE and the resulting bands were transferred to a nitrocellulose membrane with 0.2 μm pores. Membranes were subjected to Ponceau staining, incubated in 5% skim milk in PBST for 1 hour, briefly rinsed with PBST and then incubated in primary antibody solution (5% BSA in PBST or 5% skim milk in PBST) overnight at 4°C. Membranes were then washed three times, for 15 minutes each, in PBST, incubated in secondary antibody solution (1:5,000 in 5% skim milk in PBST) for 1 hour at room temperature, then washed again three times, for 15 minutes each, in PBST. Finally, chemiluminescence was detected with ECL reagents and a Biorad Chemidoc. The membranes were not stripped. The antibodies used in this study are listed in the key resources table.

**RT-qPCR—**Total RNA was isolated from cells with the Quick-RNA MicroPrep spin column kit (Zymogen, R1050), according to the manufacturer's protocol. For cDNA synthesis, we used 10 ng of total RNA for random oligomer-primed reverse transcription with Superscript II Reverse Transcriptase (Invitrogen, 18064022). Quantitative RT-PCR was carried out with the *Taq*Man Universal Master Mix (Applied Biosystems, 4305719) and *Taq*man probes for *GUSB* (4326320E), *IRF1* (Hs00971965_m1), *IFNG* (Hs00989291_m1) and *MX1* (Hs00895608_m1; Thermo Fisher Scientific).

**Deep immunophenotyping of primary leukocytes by mass cytometry (CyTOF)—**CyTOF was performed on whole blood treated with heparin ($1.0 \times 10^6$ cells per panel), with the Maxpar Direct Immune Profiling Assay (Fluidigm), according to the manufacturer's instructions. Cells were frozen at −80°C after overnight dead-cell staining. Acquisition was performed on a Helios machine (Fluidigm). All the samples were processed within 24 hours of sampling. Data were analyzed with OMIQ software.

Author Manuscript Author Manuscript Author Manuscript Author Manuscript

**Monocyte isolation and differentiation into MDMs, MDDCs and osteoclasts—** $CD14^+$ monocytes were isolated from fresh PBMCs with CD14 MicroBeads (Miltenyi Biotec, 130-050-201) according to the manufacturer's instructions. For the induction of monocyte-derived macrophages (MDMs), $CD14^+$ monocytes were cultured in RPMI 1640 supplemented with 10% FCS, 1% penicillin/streptomycin and 50 ng/ml recombinant human (rh)M-CSF (R&D Systems, 216-MC) for 7 days, and were then allowed to differentiate for seven days in the presence of 50 ng/ml rhM-CSF and 50 ng/ml rhIL-4 (R&D Systems, 204-IL). Monocyte-derived dendritic cells (MDDCs) were induced by culturing $CD14^+$ monocytes for 7 days in RPMI 1640 supplemented with 10% FCS, 1% penicillin/streptomycin, 50 ng/ml rhGM-CSF (R&D Systems, 215-GM) and 20 ng/ml rhIL-13 (R&D Systems, 213-ILB). For osteoclast differentiation, $CD14^+$ cells were cultured in $\alpha$-MEM (Thermo Fisher Scientific, 12571063) containing 10% FCS, 1% penicillin/streptomycin, 30 ng/ml rhM-CSF and 10 ng/ml rhRANKL (Peprotech, 310-01) for 7 days. The medium was replaced every three days.

**Cell-line cytokine stimulation and flow cytometry—**Cell lines were cultured as described above. For stimulation, cells were starved of IL-2 and 2% FCS overnight, as appropriate. They were then stimulated with the indicated cytokine concentrations for the indicated times at 37°C. Subsequently, for qPCR, total RNA was extracted and subjected to reverse transcription, as described above. Alternatively, dead cells were removed by Live/Dead Aqua (Thermo Fisher Scientific, L34966) staining for 5 minutes at 4°C, and the cells were then fixed and permeabilized for FACS analysis with BD Fix Buffer I and Perm Buffer III. The cells were then stained with antibodies against pSTAT1 (BD, 612564), pSTAT4 (BD, 562073) or pSTAT3 (BD, 612569) and fluorescence was assessed on a Beckman Gallios Cytometer.

**T-cell blast cytokine stimulation and RNA sequencing—**T-cell blasts were starved of IL-2 overnight. They were then stimulated with 50 ng/ml IL-12 (R&D Systems, CAT: 219-IL-005) or 100 ng/ml IL-23 (R&D Systems, Cat: 1290-IL) for 6 hours or with 2.5 ng/ml IL-1ß (R&D Systems, CAT: 201-LB-005) for 24 hours. Double-stimulated cells were stimulated with IL-1ß for 18 hours and then with IL-23 and IL-1ß for 6 hours. Total RNA was isolated from cells with the Quick-RNA MicroPrep spin-column kit (Zymogen, R1050), according to the manufacturer's protocol. RNA was then subjected to RNA-seq library preparation and deep-sequencing at the Rockefeller University Genomics Core Facility.

**The HEK-Blue IL-23 sensitive cytokine stimulation and colorimetric assay—** HEK-Blue assays were performed in accordance with the manufacturer's instructions. Briefly, HEK-Blue cells were maintained under selection with the supplier's selection compound mixture at a dilution of 1:250. For cytokine stimulations, cells were used to seed 96-well plates at a density of 25,200 cells per well, in 200 µl stimulation medium containing either without cytokines or containing 5 ng/ml IL-12, 1 ng/ml IL-23, 0.1 ng/ml IL-23 or 10.000 IU/ml IFN-α2a. After incubation for 20 hours, 20 µl culture supernatant was mixed with 180 µl QUANTI-Blue solution, incubated for 30 minutes at 37°C and then its optical density at 620-655 nm was then measured on a photometric plate reader.

Author Manuscript Author Manuscript Author Manuscript Author Manuscript

**Monocyte and NK cell sorting, culture and stimulation—**NK cells were sorted from fresh PBMCs with a BD Aria II, SORP cytometer and $CD56^+$ $CD3^-$ negative live cells were selected. This cell population was then expanded by culture in the presence of a 10-fold excess of PBMCs from the same donor irradiated with 35 grays in ImmunoCult™-XF T Cell Expansion Medium (Stem Cell Technologies, 10981) supplemented with 10 ng/ml IL-2 (Gibco, PHC0023) and 8% FCS. Before stimulation, the cells were starved of FCS and IL-2 for 20 hours. They were incubated with the indicated concentration of gandotinib for 1 hour and then treated with 100 ng/ml IL-23, 2.5 ng/ml IL-1β and/or 50 ng/ml IL-12. The purity of the NK cell preparation was assessed by flow cytometry, as illustrated in Figure S7F. Monocytes were sorted from fresh PBMCs with Miltenyi Biotec anti-CD14 magnetic microbeads in accordance with the manufacturer's instructions. They were transferred to RPMI supplemented with 10% FCS, and 1% penicillin/streptomycin and stimulated, on the same day, with gandotinib and cytokines, as described above for NK cells. IFN-α2a and IFN-γ were both used at a concentration of 10,000 IU/ml. After 24 hours, supernatants were collected and assayed by LEGENDplex bead-based ELISA.

**PBMC stimulation—**PBMCs were isolated with Lymphoprep (StemCell, 07801), from blood drawn no more than 48 hours previously into lithium heparin tubes, in accordance with the manufacturers' instructions. PBMCs were then either cryopreserved in 90% FCS, 10% DMSO or used fresh. For PBMC stimulation (fresh or cryopreserved), 100,000 PBMCs were used to seed each well of a round-bottomed 96-well plate, in RPMI supplemented with 10% human serum. They were stimulated for 48 hours with 2.5 ng/ml IL-1ß, 50 ng/ml IL-12, 100 ng/ml IL-23, 0.1 v/v% BCG or a combination of these stimuli. We added PMA (Sigma CAT: P1585-1MG, 8 ng/mL) + ionomycin (Sigma CAT: 56092-81-0, $10^{-5}$ M) for the last 24 hours only. The supernatants and cell pellets were collected. Supernatants were subjected to LEGENDplex multiplex ELISA with Human Inflammation Panel 1 (BioLegend, 740809), according to the manufacturer's instructions. Total RNA was extracted from the cell pellets for qPCR and RNA-seq analysis, as described below.

**RNA sequencing analysis—**Total RNA sequencing was performed with an Illumina NovaSeq S2 flowcell (read length 100 bp) with a read depth of 30 M. All FASTQ sequences passed quality control tests and were aligned with the GRCh38 reference genome with STAR (2.6.1d). BAM files were converted to a raw count expression matrix with featurecount. Raw count data were normalized with DEseq2. The ensemble ID targeting multiple genes was collapsed (average) and a final gene data matrix was used for a modular repertoire analysis as previously described [82,83] or for gene set enrichment analysis (GSEA: fgsea) with hallmark gene sets (http://www.gsea-msigdb.org/).

**Protein isolation from human polymorphonuclear neutrophils—**Polymorphonuclear neutrophils were isolated by density gradient centrifugation (Lymphoprep, Stem Cell Technologies) and red blood cells were lysed by incubation in red cell lysis buffer (8.02 g $NH_4Cl$, 0.84 g $NaHCO_3$, 0.37 g EDTA in 1 L $H_2O$, pH 7.4) at 37°C for 15 min. Proteins were isolated with modified RIPA buffer (25 mM Tris–HCl pH 7.4, 150 mM NaCl, 1% NP-40 and 1 mM EDTA) supplemented with DTT (0.1

Author Manuscript Author Manuscript Author Manuscript Author Manuscript

mM, Thermo Fisher Scientific), protease inhibitor cocktail (Merck), phosphatase inhibitor cocktail (Merck), PMSF (1 mM, Merck) and DFP (0.1 mM, Merck).

**Whole-blood activation and ELISA for cytokines—**Venous blood samples from healthy (local and travel) controls and patients were collected into heparin-containing collection tubes. These samples were diluted 1:2 in RPMI 1640 (GibcoBRL) supplemented with 100 IU/ml penicillin and 100 μg/ml streptomycin (GibcoBRL). We then dispensed 1 ml of each diluted blood sample into each of five wells (1 ml/well) of a 48-well plate (Nunc), which was incubated for 48 hours at 37°C, under an atmosphere containing 5% $CO_2$/95% air. The activation conditions were: medium alone, live BCG (*M. bovis*-BCG, Pasteur substrain) at a MOI of 20 BCG cells/leukocyte, BCG plus recombinant (rh) IL-12 (20 ng/ml; R&D Systems), or BCG plus IFN-γ (Imukin). The supernatants were collected after 48 hours and subjected to ELISA with the human IFN-γ, IL-12p40 (R&D) and IL-12p70 (R&D) ELISA kits, according to the manufacturer's instructions.

**VirScan - phage immunoprecipitation sequencing (PhIP-Seq)—**Antibody profiling by phage immunoprecipitation sequencing (PhIP-Seq) was performed on plasma samples from patients and controls with an expanded version of the original VirScan library, and the data were analyzed as previously described [26,103–105], but with the following modifications. We calculated species-specific significance cutoff values to estimate the minimum number of enriched, non-homologous peptides required to consider a sample seropositive, as previously described with an in-house dataset and a generalized linear model [106,107]. For each sample, we calculated virus-specific scores, by dividing the counts of enriched, non-homologous peptides by the estimated cutoff score. These adjusted virus scores are depicted on heatmap plots. We randomly selected an age-matched subset of 19 individuals from a larger cohort of 800 individuals of Arab ancestry (representing the general adult population) from our in-house database, for comparison with the patients and initial controls. Pooled human plasma used for IVIg (Privigen® CSL Behring AG), and human IgG-depleted serum (Molecular Innovations, Inc.) were used as additional controls.

**Single-cell RNA sequencing—**For scRNASeq analysis following stimulation, we analyzed cryopreserved PBMCs from six healthy controls, two MCTS1-deficient patients, two IL-23R-deficient patients and one IL-12Rβ1-deficient patient, as previously described [35,42]. Briefly, we filtered cells through a MACS SmartStrainer with 70 μm pores (Miltenyi Biotec, Cat: 130-098-462) to remove large debris, washed them three times with PBS plus 0.5% FCS, and finally filtered them through a Falcon Cell Strainer with 40 μm pores (Corning, Cat: 352340), before subjecting them to single-cell capture with the 10X Genomics Chromium chip. We prepared libraries with the Chromium Single Cell 3' Reagent Kit (v3 Chemistry) and sequenced them with an Illumina NovaSeq 6000 sequencer. We preprocessed sequences with CellRanger. We sequenced about 10,000 cells per sample. We filtered data manually on the basis of common quality-control metrics. For cell-type identification, after integration with Harmony [108] to eliminate batch-, genotype-, and stimulation-dependent variation, we performed two sequential graph-based clustering analyses. The first round of clustering identified general leukocyte subsets, whereas the second round identified memory and effector T-lymphocyte subsets and NK lymphocytes at

Author Manuscript Author Manuscript Author Manuscript Author Manuscript

sufficiently high resolution. We identified clusters with the SingleR pipeline [109] guided by the reference RNA-Seq dataset generated by Monaco et al. [110], and cell type-specific marker gene expression was then assessed manually. We visualized clusters by uniform manifold approximation and projection (UMAP). We quantified gene expression at the single-cell level with Seurat [111]. Pseudobulk analysis was performed by aggregating all reads from cells assigned to a given cluster, as previously described [112]. We performed differential expression analysis with DESeq2 [113]. We conducted geneset enrichment analysis (GSEA) with the fgsea package, by projecting the fold-change ranking onto various MSigDB genesets (http://www.gsea-msigdb.org/gsea/msigdb/genesets.jsp). All analyses were performed in R v.4 (http://www.R-project.org/). Raw data will be made available from SRA BioProject upon publication of the manuscript.

**Stimulation of PBMCs with IL-12, IL-23, BCG and PMA/ionomycin for intracellular staining and flow cytometry analysis—**This experiment was performed as previously described [34]. Healthy adult donors were recruited at the Rockefeller University (New York, USA) and Necker Hospital (Paris, France). We plated 300,000 cells per well in 96-well U-bottomed plates, at a density of 1.5 to 3 x $10^6$ cells/ml. Cells were stimulated with IL-12 (50 ng/ml), IL-23 (100 ng/ml) and/or BCG (MOI of 1) for 41 hours. For PMA plus ionomycin treatment, cells were cultured for 40 h in RPMI. They were then stimulated with 50 ng/mL PMA and 1 mM ionomycin. After 1 hour, Golgiplug was added to all cultures, in accordance with the manufacturer's protocol. Seven hours later, the cells were harvested for staining and flow cytometry. Cells were first stained with the Zombie NIR Viability kit (BioLegend) for 15 minutes. They were then stained with FcBlock (Miltenyi Biotec), anti-gdTCR-Alexa 647 (BioLegend), anti-CD3-V450 (BD Biosciences), anti-CD56-BV605 (BioLegend), anti-CD4-BUV563 (BD Biosciences), anti-Vd1TCR-FITC (Miltenyi Biotec), anti-CD8-BUV737 (BD Biosciences), anti-Vd2TCR-APC/Fire750 (BioLegend), anti-CD20-BV785 (BioLegend), anti-Va7.2-Alexa 700 (BioLegend), MR1-5-OP-RU-tetramer (NIH tetramer core facility), anti-Vb11-APC (Miltenyi Biotec), and anti-iNKT-BV480 (BD Biosciences) antibodies for 30 minutes. The stained cells were fixed with the FOXP3/Transcription Factor kit (Thermo Fisher Scientific) and subjected to intracellular staining with anti-T-bet-PE/Cy7 (BioLegend), anti-IFN-g-BV711 (BioLegend), anti-TNF-a-BV510 (BioLegend), anti-IL-17A-PERCP/Cy5.5, anti-RORgT-PE (BD Biosciences), anti-CD3-V450 (BD Biosciences), anti-CD4-BUV563 (BD Biosciences) and anti-CD8-BUV737 (BD Biosciences) antibodies in Perm/Wash buffer. Cells were then analyzed in a CyTek Aurora spectral flow cytometer.

## QUANTIFICATION AND STATISTICAL ANALYSIS

Appropriate statistical analyses were chosen depending on the experimental setting, number of replicates and type of data. The type of statistical test is always indicated in the figure legends of figure panels where statistical tests were performed. Generally, R suite was used to calculate statistical significance. All error bards in this paper display standard deviations (SD). No standard error of mean (SEM) is shown. Typically $p < 0.05$ was used as a threshold to determine statistical significance, this is always indicated in the figure legends.

Author Manuscript Author Manuscript Author Manuscript Author Manuscript

## Supplementary Material

Refer to Web version on PubMed Central for supplementary material.

## Authors

Jonathan Bohlen[1,2,3,4,@], Qinhua Zhou[5,6,#], Quentin Philippot[1,2,#], Masato Ogishi[5,#], Darawan Rinchai[5,°], Tea Nieminen[7,°], Simin Seyedpour[8,9,°], Nima Parvaneh[8,10,11,°], Nima Rezaei[8,12,°], Niloufar Yazdanpanah[8,12,°], Mana Momenilandi[1,2,°], Clément Conil[1,2,°], Anna-Lena Neehus[1,2,°], Carltin Schmidt[5,13,°], Carlos Andres Arango Franco[1,2,°], Tom Le Voyer[1,2], Taushif Khan[14,15,16], Rui Yang[5], Julia Puchan[17], Lucia Erazo[1,2], Mykola Roiuk[3,4], Taja Vatovec[1,2,4], Zarah Janda[1,2,4], Ivan Bagaric[1,2,4], Marie Materna[1,2], Adrian Gervais[1,2], Hailun Li[1,2], Jérémie Rosain[1,2], Jessica Peel[5], Yoann Seeleuthner[1,2], Ji Eun Han[5], Anne-Sophie L'Honneur[18], Marcela Moncada-Vélez[5], Marta Martin-Fernandez[19,20,21,22,23], Michael Espino Horesh[19,20,21,22,23], Tatiana Kochetkov[5], Monika Schmidt[24], Mohammed A. AlShehri[25], Eeva Salo[7], Saxen Harri[7], Gehad ElGhazali[26], Ahmad Yatim[5], Camille Soudée[1,2], Federica Sallusto[17,27], Armin Ensser[24], Nico Marr[14,15], Peng Zhang[5], Dusan Bogunovic[19,20,21,22,23], Aurélie Cobat[1,2], Mohammad Shahrooei[28,29], Vivien Béziat[1,2,5], Laurent Abel[1,2,5,§], Xiaochuan Wang[6,§], Stéphanie Boisson-Dupuis[1,2,5,§], Aurelio A. Teleman[3,4,§], Jacinta Bustamante[1,2,5,30,*,@], Qian Zhang[1,2,5,*], Jean-Laurent Casanova[1,2,5,31,32,*,@]

## Affiliations

[1]Laboratory of Human Genetics of Infectious Diseases, Necker Hospital for Sick Children, 75015 Paris, France

[2]Paris Cité University, Imagine Institute, 75015 Paris, France

[3]German Cancer Research Center (DKFZ), 69120 Heidelberg, Germany

[4]Heidelberg University, 69120 Heidelberg, Germany

[5]St. Giles Laboratory of Human Genetics of Infectious Diseases, The Rockefeller University, 10065 NY, USA

[6]Children's Hospital of Fudan University, 201102 Shanghai, China

[7]New Children's Hospital, 00290 Helsinki, Finland

[8]Research Center for Immunodeficiencies, University of Medical Sciences, P94V+8MF Tehran, Iran

[9]Nanomedicine Research Association (NRA), P94V+8MF Tehran, Iran

[10]Department of Pediatrics, Tehran University of Medical Sciences, P94V+8MF Tehran, Iran

[11]Children's Medical Center, P94V+8MF Tehran, Iran

[12]Network of Immunity in Infection, Malignancy and Autoimmunity (NIIMA), P94V+8MF Tehran, Iran

Author Manuscript Author Manuscript Author Manuscript Author Manuscript

[13]Faculty of Medicine, Heinrich Heine University Düsseldorf, 40225 Düsseldorf, Germany

[14]College of Health and Life Sciences, Hamad Bin Khalifa University, 8C8M+6Q Doha, Qatar

[15]Department of Immunology, Sidra Medicine, 8C8M+6Q Doha, Qatar

[16]The Jackson Laboratory, Farmington, CT-USA

[17]Institute of Microbiology, ETH Zürich, 8049 Zürich, Switzerland

[18]Department of Virology, Cochin Hospital, 75015 Paris, France, EU

[19]Center for Inborn Errors of Immunity, Icahn School of Medicine at Mount Sinai, 10029 NY, USA

[20]Precision Immunology Institute, Icahn School, 10029New York, NY, USA

[21]Mindich Child Health and Development Institute, Icahn School, 10029 New York, NY, USA

[22]Department of Pediatrics, Icahn School, 10029 New York, NY, USA

[23]Department of Microbiology, Icahn School, 10029 New York, NY, USA

[24]Institute of Clinical and Molecular Virology, Universitätsklinikum Erlangen, 91054 Erlangen, Germany

[25]King Fahad Medical City, Children's Specialized Hospital, 12231 Riyadh, Saudi-Arabia

[26]Sheikh Khalifa Medical City, Union71-Purehealth, United Arab Emirates University, Al Ain, United Arab Emirates

[27]Institute for Research in Biomedicine, Università della Svizzera Italiana, 6500 Bellinzona, Switzerland

[28]Clinical and Diagnostic Immunology, KU Leuven, 3000 Leuven, Belgium

[29]Dr. Shahrooei Laboratory, 22 Bahman St., Ashrafi Esfahani Blvd, Tehran, Iran

[30]Study Center for Primary Immunodeficiencies, AP-HP, 75015 Paris, France

[31]Howard Hughes Medical Institute, 10032 New York, NY, USA

[32]Department of Pediatrics, Necker Hospital, 75015 Paris, France, EU

## Acknowledgements

The authors thank all the patients, their relatives and the treatment teams for their cooperation in this study. We also thank: all the members of the HGID laboratory for helpful discussions, Christine Rivalain, Lazaro Lorenzo-Diaz, Maya Chrabieh, Mark Woollet, Erin Williams, Dana Liu and Yelena Nemirovskaya for administrative assistance. the INEM flow-cytometry facility, in particular Jerome Megret, for their support and services.

### Funding

The Laboratory of Human Genetics of Infectious Diseases was funded by the Howard Hughes Medical Institute, The Rockefeller University, the St. Giles Foundation, the National Institutes of Health (NIH) (R37AI095983), the

Author Manuscript Author Manuscript Author Manuscript Author Manuscript

National Center for Research Resources and the National Center for Advancing Sciences, NIH (UL1TR001866), the Shapiro-Silverberg Fund for the Advancement of Translational Research, the French Foundation for Medical Research (FRM) (EQU201903007798), the Integrative Biology of Emerging Infectious Diseases Laboratory of Excellence (ANR-10-LABX-62-IBEID), the French National Research Agency (ANR) under the "Investments for the future" program (ANR-10-IAHU-01), ANR-GENMSMD (ANR-16-CE17-0005-01 for J.Bu.), ANR-MAFMACRO, the European Union's Horizon 2020 research and innovation program under grant agreement no. 824110 (EASI-genomics), the Square Foundation, *Grandir - Fonds de solidarité pour l' enfance*, the SCOR Corporate Foundation for Science, *Institut National de la Santé et de la Recherche Médicale* (INSERM), and Paris Cité University. N.M. was supported by Sidra Medicine and the Qatar National Research Fund (grant no.: NPRP9-251-3-045). The Yale Center for Mendelian Genomics (UM1HG006504) was funded by the National Human Genome Research Institute, the Yale GSP Coordinating Center (U24 HG008956), and the Yale High-Performance Computing Center (S10OD018521). J.Bo. was supported by a fellowship from EMBO and a Marie Curie Research grant. M.O. was supported by the David Rockefeller Graduate Program, the Funai Foundation for Information Technology (FFIT), the Honjo International Scholarship Foundation (HISF), the New York Hideyo Noguchi Memorial Society (HNMS), and the National Cancer Institute (NCI) F99 Award (F99CA274708). Q.P. was supported by the *Assistance Publique Hopitaux de Paris* (research year) and the MD-PhD program of INSERM (*Ecole de l'INSERM Liliane Bettencourt*). J.R. was supported by the INSERM PhD program for doctors of pharmacy (*poste d'accueil* INSERM). J.R. and T.L.-V. were supported by the Bettencourt-Schueller Foundation and the MD-PhD program of the Imagine Institute. A-L.N. was supported by the Bettencourt Schueller Foundation and the International PhD program of the Imagine Institute. Q. Zhou was supported by the 'Outstanding Youth Talent Training Program' of the Children's Hospital of Fudan University.

## References

1. Casanova JL, and Abel L (2021). Lethal Infectious Diseases as Inborn Errors of Immunity: Toward a Synthesis of the Germ and Genetic Theories. Annu Rev Pathol 16, 23–50. 10.1146/annurev-pathol-031920-101429. [PubMed: 32289233]
2. Casanova JL, and Abel L (2022). From rare disorders of immunity to common determinants of infection: Following the mechanistic thread. Cell 185, 3086–3103. 10.1016/j.cell.2022.07.004. [PubMed: 35985287]
3. Furin J, Cox H, and Pai M (2019). Tuberculosis. Lancet 393, 1642–1656. 10.1016/S0140-6736(19)30308-3. [PubMed: 30904262]
4. Jouanguy E, Altare F, Lamhamedi S, Revy P, Emile JF, Newport M, Levin M, Blanche S, Seboun E, Fischer A, and Casanova JL (1996). Interferon-gamma-receptor deficiency in an infant with fatal bacille Calmette-Guerin infection. N Engl J Med 335, 1956–1961. 10.1056/NEJM199612263352604. [PubMed: 8960475]
5. Newport MJ, Huxley CM, Huston S, Hawrylowicz CM, Oostra BA, Williamson R, and Levin M (1996). A mutation in the interferon-gamma-receptor gene and susceptibility to mycobacterial infection. N Engl J Med 335, 1941–1949. 10.1056/NEJM199612263352602. [PubMed: 8960473]
6. Altare F, Durandy A, Lammas D, Emile JF, Lamhamedi S, Le Deist F, Drysdale P, Jouanguy E, Doffinger R, Bernaudin F, et al. (1998). Impairment of mycobacterial immunity in human interleukin-12 receptor deficiency. Science 280, 1432–1435. 10.1126/science.280.5368.1432. [PubMed: 9603732]
7. Altare F, Lammas D, Revy P, Jouanguy E, Doffinger R, Lamhamedi S, Drysdale P, Scheel-Toellner D, Girdlestone J, Darbyshire P, et al. (1998). Inherited interleukin 12 deficiency in a child with bacille Calmette-Guerin and Salmonella enteritidis disseminated infection. J Clin Invest 102, 2035–2040. 10.1172/JCI4950. [PubMed: 9854038]
8. Dorman SE, and Holland SM (1998). Mutation in the signal-transducing chain of the interferon-gamma receptor and susceptibility to mycobacterial infection. J Clin Invest 101, 2364–2369. 10.1172/JCI2901. [PubMed: 9616207]
9. Casanova JL, and Abel L (2002). Genetic dissection of immunity to mycobacteria: the human model. Annu Rev Immunol 20, 581–620. 10.1146/annurev.immunol.20.081501.125851. [PubMed: 11861613]
10. Casanova JL, Blanche S, Emile JF, Jouanguy E, Lamhamedi S, Altare F, Stephan JL, Bernaudin F, Bordigoni P, Turck D, et al. (1996). Idiopathic disseminated bacillus Calmette-Guerin infection: a French national retrospective study. Pediatrics 98, 774–778. [PubMed: 8885960]
11. Bustamante J. (2020). Mendelian susceptibility to mycobacterial disease: recent discoveries. Hum Genet 139, 993–1000. 10.1007/s00439-020-02120-y. [PubMed: 32025907]

Author Manuscript Author Manuscript Author Manuscript Author Manuscript


12. Bustamante J, Boisson-Dupuis S, Abel L, and Casanova JL (2014). Mendelian susceptibility to mycobacterial disease: genetic, immunological, and clinical features of inborn errors of IFN-gamma immunity. Semin Immunol 26, 454–470. 10.1016/j.smim.2014.09.008. [PubMed: 25453225]
13. Boisson-Dupuis S, and Bustamante J (2021). Mycobacterial diseases in patients with inborn errors of immunity. Curr Opin Immunol 72, 262–271. 10.1016/j.coi.2021.07.001. [PubMed: 34315005]
14. Rosain J, Kong XF, Martinez-Barricarte R, Oleaga-Quintas C, Ramirez-Alejo N, Markle J, Okada S, Boisson-Dupuis S, Casanova JL, and Bustamante J (2019). Mendelian susceptibility to mycobacterial disease: 2014-2018 update. Immunol Cell Biol 97, 360–367. 10.1111/imcb.12210. [PubMed: 30264912]
15. Martin-Fernandez M, Buta S, Le Voyer T, Li Z, Dynesen LT, Vuillier F, Franklin L, Ailal F, Muglia Amancio A, Malle L, et al. (2022). A partial form of inherited human USP18 deficiency underlies infection and inflammation. J Exp Med 219. 10.1084/jem.20211273.
16. Boisson-Dupuis S. (2020). The monogenic basis of human tuberculosis. Hum Genet 139, 1001–1009. 10.1007/s00439-020-02126-6. [PubMed: 32055999]
17. Bogunovic D, Byun M, Durfee LA, Abhyankar A, Sanal O, Mansouri D, Salem S, Radovanovic I, Grant AV, Adimi P, et al. (2012). Mycobacterial disease and impaired IFN-gamma immunity in humans with inherited ISG15 deficiency. Science 337, 1684–1688. 10.1126/science.1224026. [PubMed: 22859821]
18. Boisson-Dupuis S, Ramirez-Alejo N, Li Z, Patin E, Rao G, Kerner G, Lim CK, Krementsov DN, Hernandez N, Ma CS, et al. (2018). Tuberculosis and impaired IL-23-dependent IFN-gamma immunity in humans homozygous for a common TYK2 missense variant. Sci Immunol 3. 10.1126/sciimmunol.aau8714.
19. Bustamante J, Arias AA, Vogt G, Picard C, Galicia LB, Prando C , Grant AV, Marchal CC, Hubeau M, Chapgier A, et al. (2011). Germline CYBB mutations that selectively affect macrophages in kindreds with X-linked predisposition to tuberculous mycobacterial disease. Nat Immunol 12, 213–221. 10.1038/ni.1992. [PubMed: 21278736]
20. Dupuis S, Dargemont C, Fieschi C, Thomassin N, Rosenzweig S, Harris J, Holland SM, Schreiber RD, and Casanova JL (2001). Impairment of mycobacterial but not viral immunity by a germline human STAT1 mutation. Science 293, 300–303. 10.1126/science.1061154. [PubMed: 11452125]
21. Dupuis S, Jouanguy E, Al-Hajjar S, Fieschi C, Al-Mohsen IZ, Al-Jumaah S, Yang K, Chapgier A, Eidenschenk C, Eid P, et al. (2003). Impaired response to interferon-alpha/beta and lethal viral disease in human STAT1 deficiency. Nat Genet 33, 388–391. 10.1038/ng1097. [PubMed: 12590259]
22. Eletto D, Burns SO, Angulo I, Plagnol V, Gilmour KC, Henriquez F, Curtis J, Gaspar M, Nowak K, Daza-Cajigal V, et al. (2016). Biallelic JAK1 mutations in immunodeficient patient with mycobacterial infection. Nat Commun 7, 13992. 10.1038/ncomms13992. [PubMed: 28008925]
23. Filipe-Santos O, Bustamante J, Haverkamp MH, Vinolo E, Ku CL, Puel A, Frucht DM, Christel K, von Bernuth H, Jouanguy E, et al. (2006). X-linked susceptibility to mycobacteria is caused by mutations in NEMO impairing CD40-dependent IL-12 production. J Exp Med 203, 1745–1759. 10.1084/jem.20060085. [PubMed: 16818673]
24. Hambleton S, Salem S, Bustamante J, Bigley V, Boisson-Dupuis S, Azevedo J, Fortin A, Haniffa M, Ceron-Gutierrez L, Bacon CM, et al. (2011). IRF8 mutations and human dendritic-cell immunodeficiency. N Engl J Med 365, 127–138. 10.1056/NEJMoa1100066. [PubMed: 21524210]
25. Jouanguy E, Lamhamedi-Cherradi S, Lammas D, Dorman SE, Fondaneche MC, Dupuis S, Doffinger R, Altare F, Girdlestone J, Emile JF, et al. (1999). A human IFNGR1 small deletion hotspot associated with dominant susceptibility to mycobacterial infection. Nat Genet 21, 370–378. 10.1038/7701. [PubMed: 10192386]
26. Kerner G, Rosain J, Guerin A, Al-Khabaz A, Oleaga-Quintas C, Rapaport F, Massaad MJ, Ding JY, Khan T, Ali FA, et al. (2020). Inherited human IFN-gamma deficiency underlies mycobacterial disease. J Clin Invest 130, 3158–3171. 10.1172/JCI135460. [PubMed: 32163377]
27. Kong XF, Martinez-Barricarte R, Kennedy J, Mele F, Lazarov T, Deenick EK, Ma CS, Breton G, Lucero KB, Langlais D, et al. (2018). Disruption of an antimycobacterial circuit between dendritic and helper T cells in human SPPL2a deficiency. Nat Immunol 19, 973–985. 10.1038/s41590-018-0178-z. [PubMed: 30127434]

Author Manuscript Author Manuscript Author Manuscript Author Manuscript


28. Kreins AY, Ciancanelli MJ, Okada S, Kong XF, Ramirez-Alejo N, Kilic SS, El Baghdadi J, Nonoyama S, Mahdaviani SA, Ailal F, et al. (2015). Human TYK2 deficiency: Mycobacterial and viral infections without hyper-IgE syndrome. J Exp Med 212, 1641–1662. 10.1084/jem.20140280. [PubMed: 26304966]
29. Le Voyer T, Neehus AL, Yang R, Ogishi M, Rosain J, Alroqi F, Alshalan M, Blumental S, Al Ali F, Khan T, et al. (2021). Inherited deficiency of stress granule ZNFX1 in patients with monocytosis and mycobacterial disease. Proc Natl Acad Sci U S A 118. 10.1073/pnas.2102804118.
30. Martinez-Barricarte R, Markle JG, Ma CS, Deenick EK, Ramirez-Alejo N, Mele F, Latorre D, Mahdaviani SA, Aytekin C, Mansouri D , et al. (2018). Human IFN-gamma immunity to mycobacteria is governed by both IL-12 and IL-23. Sci Immunol 3. 10.1126/sciimmunol.aau6759.
31. Okada S, Markle JG, Deenick EK, Mele F, Averbuch D, Lagos M, Alzahrani M, Al-Muhsen S, Halwani R, Ma CS, et al. (2015). IMMUNODEFICIENCIES. Impairment of immunity to Candida and Mycobacterium in humans with bi-allelic RORC mutations. Science 349, 606–613. 10.1126/science.aaa4282. [PubMed: 26160376]
32. Vogt G, Bustamante J, Chapgier A, Feinberg J, Boisson Dupuis S, Picard C, Mahlaoui N, Gineau L, Alcais A, Lamaze C, et al. (2008). Complementation of a pathogenic IFNGR2 misfolding mutation with modifiers of N-glycosylation. J Exp Med 205, 1729–1737. 10.1084/jem.20071987. [PubMed: 18625743]
33. Vogt G, Chapgier A, Yang K, Chuzhanova N, Feinberg J, Fieschi C, Boisson-Dupuis S, Alcais A, Filipe-Santos O, Bustamante J, et al. (2005). Gains of glycosylation comprise an unexpectedly large group of pathogenic mutations. Nat Genet 37, 692–700. 10.1038/ng1581. [PubMed: 15924140]
34. Yang R, Mele F, Worley L, Langlais D, Rosain J, Benhsaien I, Elarabi H, Croft CA, Doisne JM, Zhang P, et al. (2020). Human T-bet Governs Innate and Innate-like Adaptive IFN-gamma Immunity against Mycobacteria. Cell 183, 1826–1847 e1831. 10.1016/j.cell.2020.10.046. [PubMed: 33296702]
35. Ogishi M, Arias AA, Yang R, Han JE, Zhang P, Rinchai D, Halpern J, Mulwa J, Keating N, Chrabieh M, et al. (2022). Impaired IL-23-dependent induction of IFN-gamma underlies mycobacterial disease in patients with inherited TYK2 deficiency. J Exp Med 219. 10.1084/jem.20220094.
36. Rosain J, Neehus AL, Manry J, Yang R, Le Pen J, Daher W, Liu Z, Chan YH, Tahuil N, Turel O, et al. (2023). Human IRF1 governs macrophagic IFN-gamma immunity to mycobacteria. Cell 186, 621–645 e633. 10.1016/j.cell.2022.12.038. [PubMed: 36736301]
37. Doffinger R, Jouanguy E, Dupuis S, Fondaneche MC, Stephan JL, Emile JF, Lamhamedi-Cherradi S, Altare F, Pallier A, Barcenas-Morales G, et al. (2000). Partial interferon-gamma receptor signaling chain deficiency in a patient with bacille Calmette-Guerin and Mycobacterium abscessus infection. J Infect Dis 181, 379–384. 10.1086/315197. [PubMed: 10608793]
38. de Beaucoudrey L, Samarina A, Bustamante J, Cobat A, Boisson-Dupuis S, Feinberg J, Al-Muhsen S, Janniere L, Rose Y, de Suremain M, et al. (2010). Revisiting human IL-12Rbeta1 deficiency: a survey of 141 patients from 30 countries. Medicine (Baltimore) 89, 381–402. 10.1097/MD.0b013e3181fdd832. [PubMed: 21057261]
39. Fieschi C, Dupuis S, Catherinot E, Feinberg J, Bustamante J, Breiman A, Altare F, Baretto R, Le Deist F, Kayal S, et al. (2003). Low penetrance, broad resistance, and favorable outcome of interleukin 12 receptor beta1 deficiency: medical and immunological implications. J Exp Med 197, 527–535. 10.1084/jem.20021769. [PubMed: 12591909]
40. Rosain J, Oleaga-Quintas C, Deswarte C, Verdin H, Marot S, Syridou G, Mansouri M, Mahdaviani SA, Venegas-Montoya E, Tsolia M, et al. (2018). A Variety of Alu-Mediated Copy Number Variations Can Underlie IL-12Rbeta1 Deficiency. J Clin Immunol 38, 617–627. 10.1007/s10875-018-0527-6. [PubMed: 29995221]
41. Staels F, Lorenzetti F, De Keukeleere K, Willemsen M, Gerbaux M, Neumann J, Tousseyn T, Pasciuto E, De Munter P, Bossuyt X, et al. (2022). A Novel Homozygous Stop Mutation in IL23R Causes Mendelian Susceptibility to Mycobacterial Disease. J Clin Immunol. 10.1007/s10875-022-01320-7.
42. Philippot Q, Ogishi M, Bohlen J, Puchan J, Arias AA, Nguyen T, Martin-Fernandez M, Conil C, Rinchai D, Momenilandi M, et al. (2023). Human IL-23 is essential for IFN-gamma-dependent

Author Manuscript Author Manuscript Author Manuscript Author Manuscript

immunity to mycobacteria. Sci Immunol 8, eabq5204. 10.1126/sciimmunol.abq5204. [PubMed: 36763636]

43. Nathan CF, Murray HW, Wiebe ME, and Rubin BY (1983). Identification of interferon-gamma as the lymphokine that activates human macrophage oxidative metabolism and antimicrobial activity. J Exp Med 158, 670–689. 10.1084/jem.158.3.670. [PubMed: 6411853]
44. Vogt G, and Nathan C (2011). In vitro differentiation of human macrophages with enhanced antimycobacterial activity. J Clin Invest 121, 3889–3901. 10.1172/JCI57235. [PubMed: 21911939]
45. Levy R, Langlais D, Beziat V, Rapaport F, Rao G, Lazarov T, Bourgey M, Zhou YJ, Briand C, Moriya K, et al. (2021). Inherited human c-Rel deficiency disrupts myeloid and lymphoid immunity to multiple infectious agents. J Clin Invest 131. 10.1172/JCI150143.
46. Rosain J, Bernasconi A, Prieto E, Caputi L, Le Voyer T, Buda G, Marti M, Bohlen J, Neehus AL, Castanos C, et al. (2022). Pulmonary Alveolar Proteinosis and Multiple Infectious Diseases in a Child with Autosomal Recessive Complete IRF8 Deficiency. J Clin Immunol 42, 975–985. 10.1007/s10875-022-01250-4. [PubMed: 35338423]
47. Cytlak U, Resteu A, Pagan S, Green K, Milne P, Maisuria S, McDonald D, Hulme G, Filby A, Carpenter B, et al. (2020). Differential IRF8 Transcription Factor Requirement Defines Two Pathways of Dendritic Cell Development in Humans. Immunity 53, 353–370 e358. 10.1016/j.immuni.2020.07.003. [PubMed: 32735845]
48. Villani AC, Satija R, Reynolds G, Sarkizova S, Shekhar K, Fletcher J, Griesbeck M, Butler A, Zheng S, Lazo S, et al. (2017). Single-cell RNA-seq reveals new types of human blood dendritic cells, monocytes, and progenitors. Science 356. 10.1126/science.aah4573.
49. Casanova JL, and Abel L (2004). The human model: a genetic dissection of immunity to infection in natural conditions. Nat Rev Immunol 4, 55–66. 10.1038/nri1264. [PubMed: 14704768]
50. Medetgul-Ernar K, and Davis MM (2022). Standing on the shoulders of mice. Immunity 55, 1343–1353. 10.1016/j.immuni.2022.07.008. [PubMed: 35947979]
51. Wheelock EF (1965). Interferon-like virus-inhibitor induced in human leukocytes by phytohemagglutinin. Science 149, 310–311.
52. Daza-Cajigal V, Albuquerque AS, Young DF, Ciancanelli MJ, Moulding D, Angulo I, Jeanne-Julien V, Rosain J, Minskaia E, Casanova JL, et al. (2022). Partial human Janus kinase 1 deficiency predominantly impairs responses to interferon gamma and intracellular control of mycobacteria. Front Immunol 13, 888427. 10.3389/fimmu.2022.888427. [PubMed: 36159783]
53. Khanolkar A, Kirschmann DA, Caparelli EA, Wilks JD, Cerullo JM, Bergerson JRE, Jennings LJ, and Fuleihan RL (2018). CD4 T cell-restricted IL-2 signaling defect in a patient with a novel IFNGR1 deficiency. J Allergy Clin Immunol 141, 435–439 e437. 10.1016/j.jaci.2017.08.018. [PubMed: 28927822]
54. Kerner G, Ramirez-Alejo N, Seeleuthner Y, Yang R, Ogishi M, Cobat A, Patin E, Quintana-Murci L, Boisson-Dupuis S, Casanova JL, and Abel L (2019). Homozygosity for TYK2 P1104A underlies tuberculosis in about 1% of patients in a cohort of European ancestry. Proc Natl Acad Sci U S A 116, 10430–10434. 10.1073/pnas.1903561116. [PubMed: 31068474]
55. Itan Y, Shang L, Boisson B, Ciancanelli MJ, Markle JG, Martinez-Barricarte R, Scott E, Shah I, Stenson PD, Gleeson J, et al. (2016). The mutation significance cutoff: gene-level thresholds for variant predictions. Nat Methods 13, 109–110. 10.1038/nmeth.3739. [PubMed: 26820543]
56. Kircher M, Witten DM, Jain P, O'Roak BJ, Cooper GM, and Shendure J (2014). A general framework for estimating the relative pathogenicity of human genetic variants. Nat Genet 46, 310–315. 10.1038/ng.2892. [PubMed: 24487276]
57. Rapaport F, Boisson B, Gregor A, Beziat V, Boisson-Dupuis S, Bustamante J, Jouanguy E, Puel A, Rosain J, Zhang Q, et al. (2021). Negative selection on human genes underlying inborn errors depends on disease outcome and both the mode and mechanism of inheritance. Proc Natl Acad Sci U S A 118. 10.1073/pnas.2001248118.
58. Schleich S, Strassburger K, Janiesch PC, Koledachkina T, Miller KK, Haneke K, Cheng YS, Kuechler K, Stoecklin G, Duncan KE, and Teleman AA (2014). DENR-MCT-1 promotes translation reinitiation downstream of uORFs to control tissue growth. Nature 512, 208–212. 10.1038/nature13401. [PubMed: 25043021]

Author Manuscript Author Manuscript Author Manuscript Author Manuscript


59. Bohlen J, Harbrecht L, Blanco S, Clemm von Hohenberg K, Fenzl K, Kramer G, Bukau B, and Teleman AA (2020). DENR promotes translation reinitiation via ribosome recycling to drive expression of oncogenes including ATF4. Nat Commun 11, 4676. 10.1038/s41467-020-18452-2. [PubMed: 32938922]
60. Dickinson ME, Flenniken AM, Ji X, Teboul L, Wong MD, White JK, Meehan TF, Weninger WJ, Westerberg H, Adissu H, et al. (2016). High-throughput discovery of novel developmental phenotypes. Nature 537, 508–514. 10.1038/nature19356. [PubMed: 27626380]
61. Uhlen M, Fagerberg L, Hallstrom BM, Lindskog C, Oksvold P, Mardinoglu A, Sivertsson A, Kampf C, Sjostedt E, Asplund A, et al. (2015). Proteomics. Tissue-based map of the human proteome. Science 347, 1260419. 10.1126/science.1260419. [PubMed: 25613900]
62. Schleich S, Acevedo JM, Clemm von Hohenberg K, and Teleman AA (2017). Identification of transcripts with short stuORFs as targets for DENR*MCTS1-dependent translation in human cells. Sci Rep 7, 3722. 10.1038/s41598-017-03949-6. [PubMed: 28623304]
63. Lizio M, Abugessaisa I, Noguchi S, Kondo A, Hasegawa A, Hon CC, de Hoon M, Severin J, Oki S, Hayashizaki Y, et al. (2019). Update of the FANTOM web resource: expansion to provide additional transcriptome atlases. Nucleic Acids Res 47, D752–D758. 10.1093/nar/gky1099. [PubMed: 30407557]
64. Lizio M, Harshbarger J, Shimoji H, Severin J, Kasukawa T, Sahin S, Abugessaisa I, Fukuda S, Hori F, Ishikawa-Kato S, et al. (2015). Gateways to the FANTOM5 promoter level mammalian expression atlas. Genome Biol 16, 22. 10.1186/s13059-014-0560-6. [PubMed: 25723102]
65. Bohlen J, Fenzl K, Kramer G, Bukau B, and Teleman AA (2020). Selective 40S Footprinting Reveals Cap-Tethered Ribosome Scanning in Human Cells. Mol Cell 79, 561–574 e565. 10.1016/j.molcel.2020.06.005. [PubMed: 32589966]
66. Wagner S, Bohlen J, Herrmannova A, Jelinek J, Preiss T, Valasek LS, and Teleman AA (2022). Selective footprinting of 40S and 80S ribosome subpopulations (Sel-TCP-seq) to study translation and its control. Nat Protoc. 10.1038/s41596-022-00708-4.
67. Young DJ, Makeeva DS, Zhang F, Anisimova AS, Stolboushkina EA, Ghobakhlou F, Shatsky IN, Dmitriev SE, Hinnebusch AG, and Guydosh NR (2018). Tma64/eIF2D, Tma20/MCT-1, and Tma22/DENR Recycle Post-termination 40S Subunits In Vivo. Mol Cell 71, 761–774 e765. 10.1016/j.molcel.2018.07.028. [PubMed: 30146315]
68. Xiao Z, Zou Q, Liu Y, and Yang X (2016). Genome-wide assessment of differential translations with ribosome profiling data. Nat Commun 7, 11194. 10.1038/ncomms11194. [PubMed: 27041671]
69. Clemm von Hohenberg K, Muller S, Schleich S, Meister M, Bohlen J, Hofmann TG, and Teleman AA (2022). Cyclin B/CDK1 and Cyclin A/CDK2 phosphorylate DENR to promote mitotic protein translation and faithful cell division. Nat Commun 13, 668. 10.1038/s41467-022-28265-0. [PubMed: 35115540]
70. Neubauer H, Cumano A, Muller M, Wu H, Huffstadt U, and Pfeffer K (1998). Jak2 deficiency defines an essential developmental checkpoint in definitive hematopoiesis. Cell 93, 397–409. 10.1016/s0092-8674(00)81168-x. [PubMed: 9590174]
71. Morris R, Kershaw NJ, and Babon JJ (2018). The molecular details of cytokine signaling via the JAK/STAT pathway. Protein Sci 27, 1984–2009. 10.1002/pro.3519. [PubMed: 30267440]
72. Macchi P, Villa A, Giliani S, Sacco MG, Frattini A, Porta F, Ugazio AG, Johnston JA, Candotti F, O'Shea JJ, and et al. (1995). Mutations of Jak-3 gene in patients with autosomal severe combined immune deficiency (SCID). Nature 377, 65–68. 10.1038/377065a0. [PubMed: 7659163]
73. Teng MW, Bowman EP, McElwee JJ, Smyth MJ, Casanova JL, Cooper AM, and Cua DJ (2015). IL-12 and IL-23 cytokines: from discovery to targeted therapies for immune-mediated inflammatory diseases. Nat Med 21, 719–729. 10.1038/nm.3895. [PubMed: 26121196]
74. Igarashi K, Garotta G, Ozmen L, Ziemiecki A, Wilks AF, Harpur AG, Larner AC, and Finbloom DS (1994). Interferon-gamma induces tyrosine phosphorylation of interferon-gamma receptor and regulated association of protein tyrosine kinases, Jak1 and Jak2, with its receptor. J Biol Chem 269, 14333–14336. [PubMed: 7514165]

Author Manuscript Author Manuscript Author Manuscript Author Manuscript


75. Silva CM, Lu H, Weber MJ, and Thorner MO (1994). Differential tyrosine phosphorylation of JAK1, JAK2, and STAT1 by growth hormone and interferon-gamma in IM-9 cells. J Biol Chem 269, 27532–27539. [PubMed: 7525556]
76. Sun R, and Abraham C (2020). IL23 Promotes Antimicrobial Pathways in Human Macrophages, Which Are Reduced With the IBD-Protective IL23R R381Q Variant. Cell Mol Gastroenterol Hepatol 10, 673–697. 10.1016/j.jcmgh.2020.05.007. [PubMed: 32474165]
77. Hammaren HM, Virtanen AT, Raivola J, and Silvennoinen O (2019). The regulation of JAKs in cytokine signaling and its breakdown in disease. Cytokine 118, 48–63. 10.1016/j.cyto.2018.03.041. [PubMed: 29685781]
78. Ma L, Clayton JR, Walgren RA, Zhao B, Evans RJ, Smith MC, Heinz-Taheny KM, Kreklau EL, Bloem L, Pitou C, et al. (2013). Discovery and characterization of LY2784544, a small-molecule tyrosine kinase inhibitor of JAK2V617F. Blood Cancer J 3, e109. 10.1038/bcj.2013.6. [PubMed: 23584399]
79. Fieschi C, Dupuis S, Picard C, Smith CI, Holland SM, and Casanova JL (2001). High levels of interferon gamma in the plasma of children with complete interferon gamma receptor deficiency. Pediatrics 107, E48. 10.1542/peds.107.4.e48. [PubMed: 11335769]
80. Suzuki T, Sakagami T, Rubin BK, Nogee LM, Wood RE, Zimmerman SL, Smolarek T, Dishop MK, Wert SE, Whitsett JA, et al. (2008). Familial pulmonary alveolar proteinosis caused by mutations in CSF2RA. J Exp Med 205, 2703–2710. 10.1084/jem.20080990. [PubMed: 18955570]
81. Suzuki T, Sakagami T, Young LR, Carey BC, Wood RE, Luisetti M, Wert SE, Rubin BK, Kevill K, Chalk C, et al. (2010). Hereditary pulmonary alveolar proteinosis: pathogenesis, presentation, diagnosis, and therapy. Am J Respir Crit Care Med 182, 1292–1304. 10.1164/rccm.201002-0271OC. [PubMed: 20622029]
82. Altman MC, Rinchai D, Baldwin N, Toufiq M, Whalen E, Garand M, Syed Ahamed Kabeer B, Alfaki M, Presnell SR, Khaenam P, et al. (2021). Development of a fixed module repertoire for the analysis and interpretation of blood transcriptome data. Nat Commun 12, 4385. 10.1038/s41467-021-24584-w. [PubMed: 34282143]
83. Rinchai D, Roelands J, Toufiq M, Hendrickx W, Altman MC, Bedognetti D, and Chaussabel D (2021). BloodGen3Module: Blood transcriptional module repertoire analysis and visualization using R. Bioinformatics. 10.1093/bioinformatics/btab121.
84. Schoenborn JR, and Wilson CB (2007). Regulation of interferon-gamma during innate and adaptive immune responses. Adv Immunol 96, 41–101. 10.1016/S0065-2776(07)96002-2. [PubMed: 17981204]
85. Chen B, Hu J, Hu X, Chen H, Bao R, Zhou Y, Ye Y, Zhan M, Cai W, Li H, and Li HB (2022). DENR controls JAK2 translation to induce PD-L1 expression for tumor immune evasion. Nat Commun 13, 2059. 10.1038/s41467-022-29754-y. [PubMed: 35440133]
86. Glassman CR, Mathiharan YK, Jude KM, Su L, Panova O, Lupardus PJ, Spangler JB, Ely LK, Thomas C, Skiniotis G, and Garcia KC (2021). Structural basis for IL-12 and IL-23 receptor sharing reveals a gateway for shaping actions on T versus NK cells. Cell 184, 983–999 e924. 10.1016/j.cell.2021.01.018. [PubMed: 33606986]
87. Hummel TM, Ackfeld T, Schonberg M, Ciupka G, Schulz F, Oberdoerster A, Grotzinger J, Scheller J, and Floss DM (2017). Synthetic Deletion of the Interleukin 23 Receptor (IL-23R) Stalk Region Led to Autonomous IL-23R Homodimerization and Activation. Mol Cell Biol 37. 10.1128/MCB.00014-17.
88. Cua DJ, Sherlock J, Chen Y, Murphy CA, Joyce B, Seymour B, Lucian L, To W, Kwan S, Churakova T, et al. (2003). Interleukin-23 rather than interleukin-12 is the critical cytokine for autoimmune inflammation of the brain. Nature 421, 744–748. 10.1038/nature01355. [PubMed: 12610626]
89. Gaffen SL, Jain R, Garg AV, and Cua DJ (2014). The IL-23-IL-17 immune axis: from mechanisms to therapeutic testing. Nat Rev Immunol 14, 585–600. 10.1038/nri3707. [PubMed: 25145755]
90. Steinman L (2007). A brief history of T(H)17, the first major revision in the T(H)1/T(H)2 hypothesis of T cell-mediated tissue damage. Nat Med 13, 139–145. 10.1038/nm1551. [PubMed: 17290272]

Author Manuscript Author Manuscript Author Manuscript Author Manuscript

91. Fieschi C, and Casanova JL (2003). The role of interleukin-12 in human infectious diseases: only a faint signature. Eur J Immunol 33, 1461–1464. 10.1002/eji.200324038. [PubMed: 12778462]

92. Acosta-Rodriguez EV, Rivino L, Geginat J, Jarrossay D, Gattorno M, Lanzavecchia A, Sallusto F, and Napolitani G (2007). Surface phenotype and antigenic specificity of human interleukin 17-producing T helper memory cells. Nat Immunol 8, 639–646. 10.1038/ni1467. [PubMed: 17486092]

93. Zielinski CE, Corti D, Mele F, Pinto D, Lanzavecchia A, and Sallusto F (2011). Dissecting the human immunologic memory for pathogens. Immunol Rev 240, 40–51. 10.1111/j.1600-065X.2010.01000.x. [PubMed: 21349085]

94. Lindestam Arlehamn CS, Gerasimova A, Mele F, Henderson R, Swann J, Greenbaum JA, Kim Y, Sidney J, James EA, Taplitz R, et al. (2013). Memory T cells in latent Mycobacterium tuberculosis infection are directed against three antigenic islands and largely contained in a CXCR3+CCR6+ Th1 subset. PLoS Pathog 9, e1003130. 10.1371/journal.ppat.1003130. [PubMed: 23358848]

95. Lander ES, Linton LM, Birren B, Nusbaum C, Zody MC, Baldwin J, Devon K, Dewar K, Doyle M, FitzHugh W, et al. (2001). Initial sequencing and analysis of the human genome. Nature 409, 860–921. 10.1038/35057062. [PubMed: 11237011]

96. Li H, and Durbin R (2009). Fast and accurate short read alignment with Burrows-Wheeler transform. Bioinformatics 25, 1754–1760. 10.1093/bioinformatics/btp324. [PubMed: 19451168]

97. Van der Auwera, G.O.C. B, (2020). Genomics in the Cloud: Using Docker, GATK, and WDL in Terra (1st Edition). O'Reilly Media.

98. Cingolani P, Platts A, Wang le L, Coon M, Nguyen T, Wang L, Land SJ, Lu X, and Ruden DM (2012). A program for annotating and predicting the effects of single nucleotide polymorphisms, SnpEff: SNPs in the genome of Drosophila melanogaster strain w1118; iso-2; iso-3. Fly (Austin) 6, 80–92. 10.4161/fly.19695. [PubMed: 22728672]

99. D. F, (1993). Bias reduction of maximum likelihood estimates Biometrika, 27–38.

100. Team, R.C. (2022). R: A language and environment for statistical computing. . R Foundation for Statistical Computing, Vienna, Austria.

101. Wagner S, Bohlen J, Herrmannova A, Jelinek J, Preiss T, Valasek LS, and Teleman AA (2022). Selective footprinting of 40S and 80S ribosome subpopulations (Sel-TCP-seq) to study translation and its control. Nat Protoc 17, 2139–2187. 10.1038/s41596-022-00708-4. [PubMed: 35869369]

102. Langmead B, and Salzberg SL (2012). Fast gapped-read alignment with Bowtie 2. Nature methods 9, 357–359. 10.1038/nmeth.1923. [PubMed: 22388286]

103. Drutman SB, Mansouri D, Mahdaviani SA, Neehus AL, Hum D, Bryk R, Hernandez N, Belkaya S, Rapaport F, Bigio B, et al. (2020). Fatal Cytomegalovirus Infection in an Adult with Inherited NOS2 Deficiency. N Engl J Med 382, 437–445. 10.1056/NEJMoa1910640. [PubMed: 31995689]

104. Mina MJ, Kula T, Leng Y, Li M, de Vries RD, Knip M, Siljander H, Rewers M, Choy DF, Wilson MS, et al. (2019). Measles virus infection diminishes preexisting antibodies that offer protection from other pathogens. Science 366, 599–606. 10.1126/science.aay6485. [PubMed: 31672891]

105. Mohan D, Wansley DL, Sie BM, Noon MS, Baer AN, Laserson U, and Larman HB (2019). Publisher Correction: PhIP-Seq characterization of serum antibodies using oligonucleotide-encoded peptidomes. Nat Protoc 14, 2596. 10.1038/s41596-018-0088-4.

106. Hasan MR, Rahman M, Khan T, Saeed A, Sundararaju S, Flores A, Hawken P, Rawat A, Elkum N, Hussain K, et al. (2021). Virome-wide serological profiling reveals association of herpesviruses with obesity. Sci Rep 11, 2562. 10.1038/s41598-021-82213-4. [PubMed: 33510449]

107. Khan T, Rahman M, Ali FA, Huang SSY, Ata M, Zhang Q, Bastard P, Liu Z, Jouanguy E, Beziat V, et al. (2021). Distinct antibody repertoires against endemic human coronaviruses in children and adults. JCI Insight 6. 10.1172/jci.insight.144499.

108. Korsunsky I, Millard N, Fan J, Slowikowski K, Zhang F, Wei K, Baglaenko Y, Brenner M, Loh PR, and Raychaudhuri S (2019). Fast, sensitive and accurate integration of single-cell data with Harmony. Nat Methods 16, 1289–1296. 10.1038/s41592-019-0619-0. [PubMed: 31740819]

109. Aran D, Looney AP, Liu L, Wu E, Fong V, Hsu A, Chak S, Naikawadi RP, Wolters PJ, Abate AR, et al. (2019). Reference-based analysis of lung single-cell sequencing reveals a

Author Manuscript Author Manuscript Author Manuscript Author Manuscript

transitional profibrotic macrophage. Nat Immunol 20, 163–172. 10.1038/s41590-018-0276-y. [PubMed: 30643263]

110. Monaco G, Lee B, Xu W, Mustafah S, Hwang YY, Carre C, Burdin N, Visan L, Ceccarelli M, Poidinger M, et al. (2019). RNA-Seq Signatures Normalized by mRNA Abundance Allow Absolute Deconvolution of Human Immune Cell Types. Cell Rep 26, 1627–1640 e1627. 10.1016/j.celrep.2019.01.041. [PubMed: 30726743]
111. Hao Y, Hao S, Andersen-Nissen E, Mauck WM 3rd, Zheng S, Butler A, Lee MJ, Wilk AJ, Darby C, Zager M, et al. (2021). Integrated analysis of multimodal single-cell data. Cell 184, 3573–3587 e3529. 10.1016/j.cell.2021.04.048. [PubMed: 34062119]
112. Crowell HL, Soneson C, Germain PL, Calini D, Collin L, Raposo C, Malhotra D, and Robinson MD (2020). muscat detects subpopulation-specific state transitions from multi-sample multi-condition single-cell transcriptomics data. Nat Commun 11, 6077. 10.1038/s41467-020-19894-4. [PubMed: 33257685]
113. Love MI, Huber W, and Anders S (2014). Moderated estimation of fold change and dispersion for RNA-seq data with DESeq2. Genome Biol 15, 550. 10.1186/s13059-014-0550-8. [PubMed: 25516281]

Author Manuscript Author Manuscript Author Manuscript Author Manuscript

## Highlights

- X-linked recessive complete human MCTS1 deficiency underlies mycobacterial disease
- A lack of MCTS1 inhibits JAK2 translation by impairing ribosome recycling at two uORFs
- Decreases in JAK2 protein levels impair the responses of NK and T lymphocytes to IL-23
- Innate-like T cells from patients produce low levels of IFN-γ upon IL-23 stimulation

Author Manuscript Author Manuscript Author Manuscript Author Manuscript

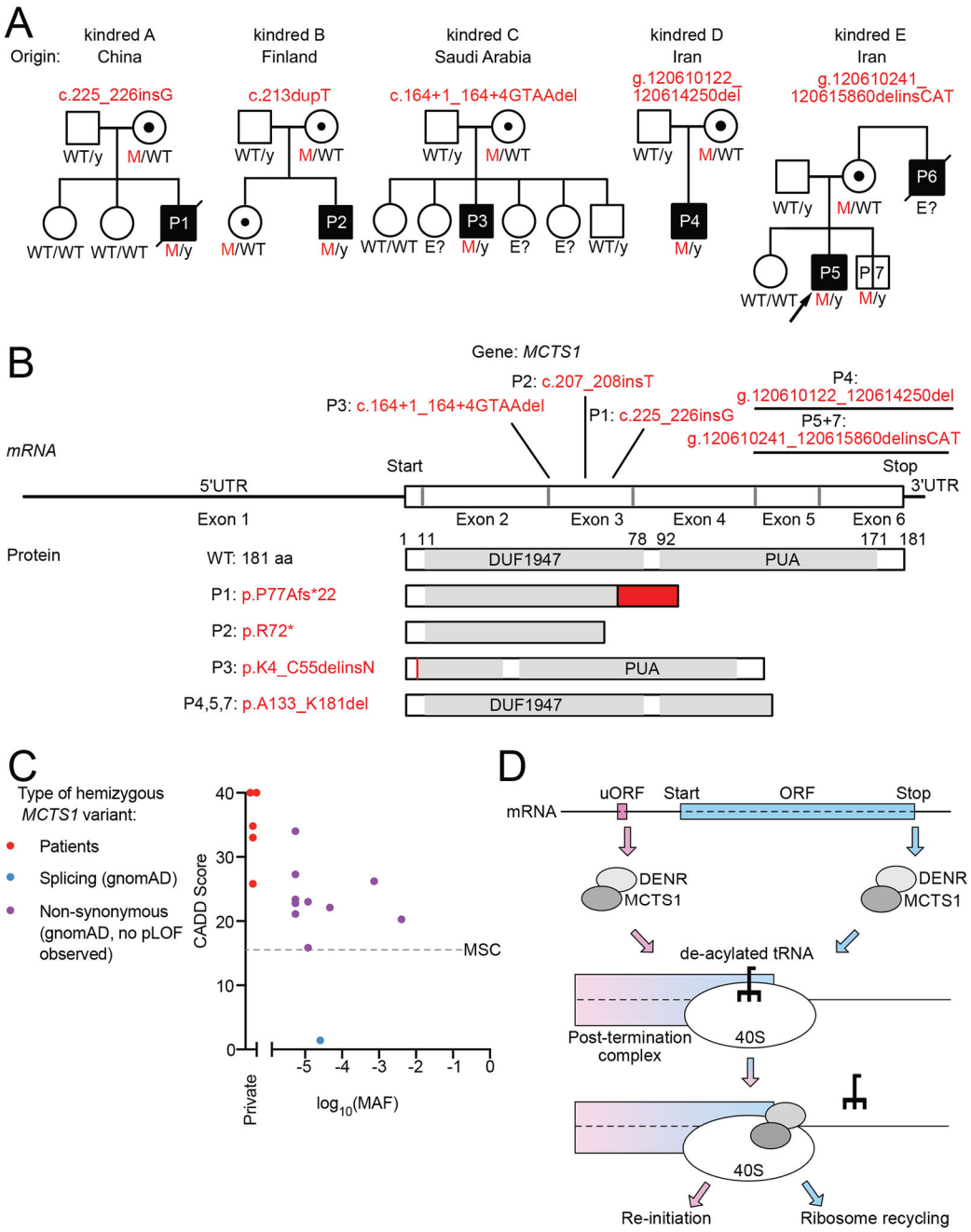


**Figure 1: Hemizygous *MCTS1* mutations in patients with MSMD from five unrelated families.**

**(A)** Family pedigrees with allele segregation. The patients in black suffer from MSMD and are hemizygous for the indicated *MCTS1* alleles. The arrow indicates the proband. Other symbols; asymptomatic: black vertical line, heterozygous: blackdots, unknown genotype: "E?", wild-type: WT. **(B)** Schematic representation of the MCTS1 mRNA (top) and protein (middle) structure. (Bottom) Predicted protein products of the *MCTS1* variants found in MSMD patients. **(C)** CADD MAF plot of all the nonsynonymous, hemizygous *MCTS1* variants of the gnomAD database (in black, splicing in blue), and the five *MCTS1* pLOF

Author Manuscript Author Manuscript Author Manuscript Author Manuscript

variants of patients with MSMD (in red). **(D)** Schematic representation of the known molecular function of MCTS1 and its binding partner, DENR.

Author Manuscript Author Manuscript Author Manuscript Author Manuscript

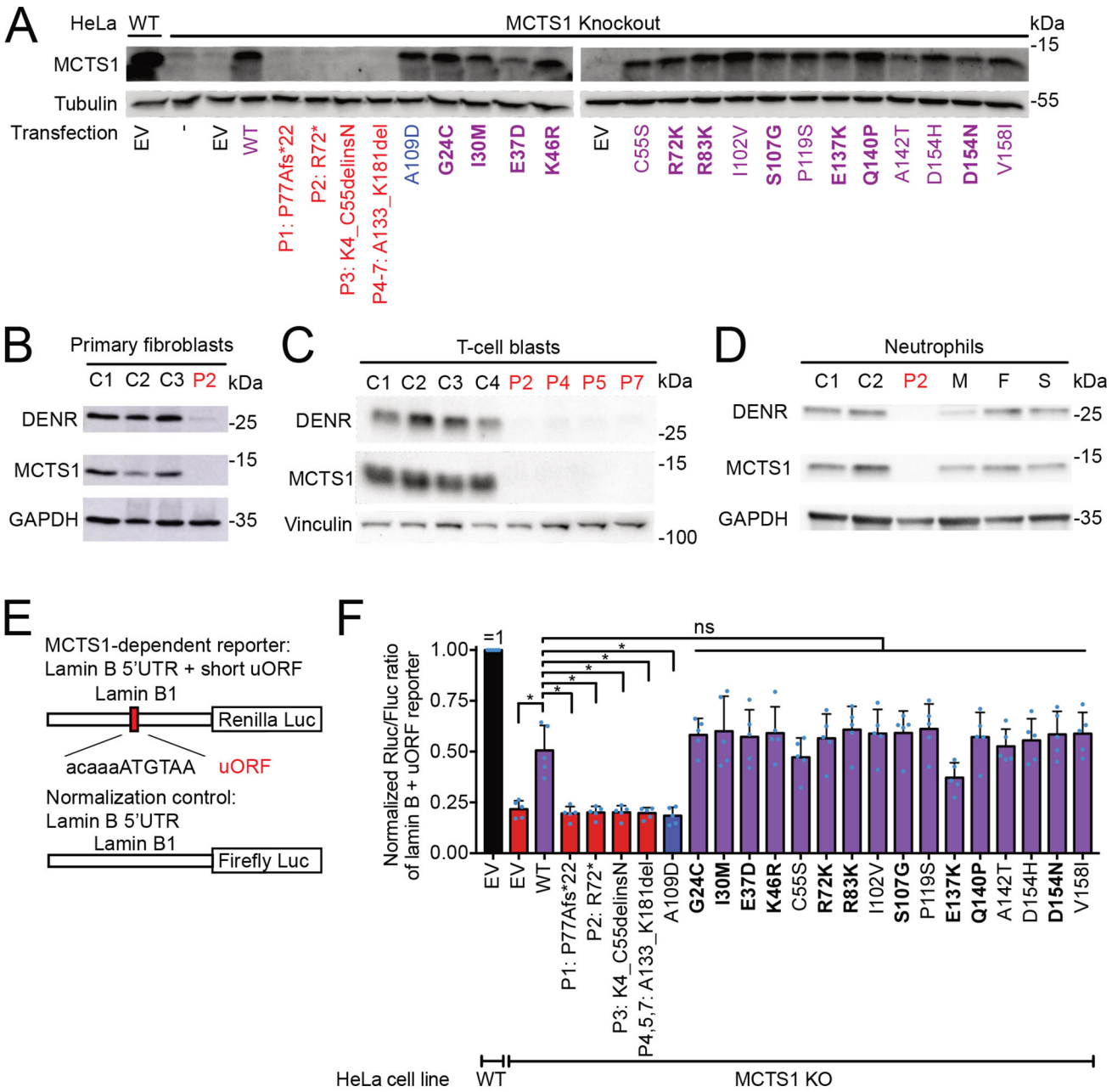


**Figure 2: The *MCTS1* mutations found in MSMD patients are loss-of-expression and loss-of-function.**

**(A)** Western blot of wild-type (WT) and MCTS1$^{KO}$ HeLa cells transiently transfected with MCTS1 variants; Red: patients; blue: synthetic LOF variant; purple: gnomAD missense variants; EV: empty vector. Bold variants: hemizygous in gnomAD. Representative data from three independent experiments are shown. **(B-D)** Levels of MCTS1 protein in **(B)** primary fibroblasts from P2 and healthy controls, **(C)** T-cell blasts from P2, P4, P5 and P7 and healthy WT controls, and **(D)** neutrophils of P2, his relatives (M = mother, F= father, S = sister) and two healthy WT controls (C1, C2) as determined by western blotting. **(E)** Schematic representation of the reporter constructs used for the MCTS1 activity assay in

Author Manuscript Author Manuscript Author Manuscript Author Manuscript

**(F)** Activity of the MCTS1 variants used for the transient transfection of MCTS1$^{KO}$ HeLa cells, as assessed by the luciferase translation reinitiation assay. Bars: mean and SD of five biological replicates. Statistical significance was assessed in unpaired Welch's *t*-tests corrected for multiple testing. *$p$<0.05

Author Manuscript Author Manuscript Author Manuscript Author Manuscript

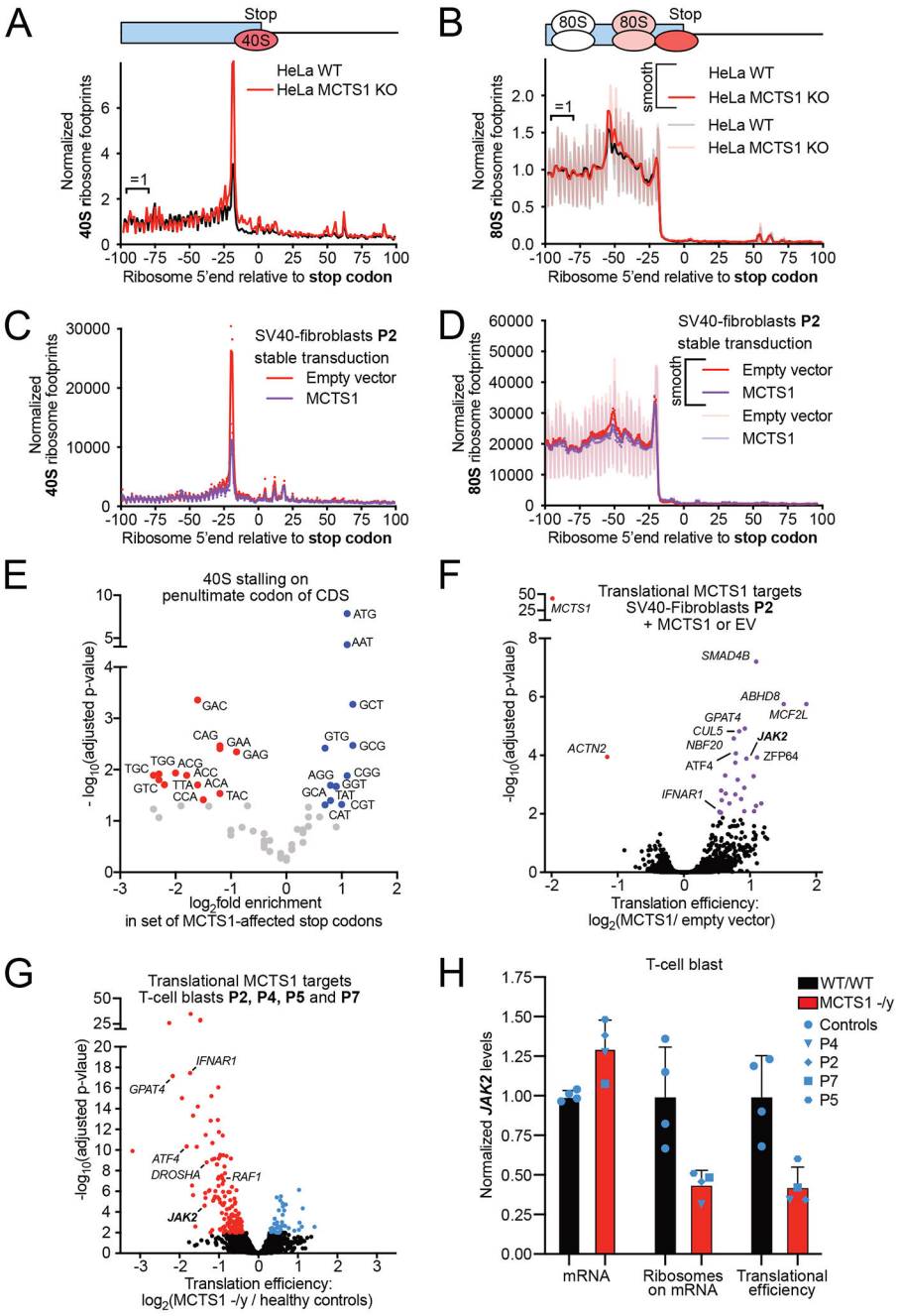


**Figure 3: Defective ribosome recycling and translation reinitiation in the patients' cells**

**(A-D)** Metagene profiles for 40S **(A, C)** and 80S **(B, D)** ribosome footprinting showing the position of the 5' end of the ribosome footprints relative to the stop codons of all proteins (coding ORFs) in HeLa cells **(A, B)** and SV40-fibroblasts **(C, D). (A, B)** Read counts normalized against the area indicated on the plot; **(C, D)** Read counts normalized by sequencing depth. **(E)** Penultimate codon enrichments for mORFs in the top quartile for 40S accumulation ($n$ = 1034) relative to all detected mORF stop codons ($n$ = 4222). Significance was assessed in binomial tests, with correction for multiple testing. **(F)** Volcano

Author Manuscript Author Manuscript Author Manuscript Author Manuscript

plot of changes in translation efficiency from 80S footprinting data for P2 SV40-fibroblasts +/− MCTS1. The *p*-values adjusted for multiple testing in X-tail analysis are shown on the *y*-axis. **(G)** Volcano plot of changes in translation efficiency from the 80S footprinting data of T-cell blasts from P2, P4, P5, P7 relative to four healthy controls. The *p*-values adjusted for multiple testing by X-tail analysis are shown on the *y*-axis. **(H)** Levels of mRNA, ribosome footprints on mRNA and translation efficiency for the *JAK2* endogenous mRNA from **(G)**.

Author Manuscript Author Manuscript Author Manuscript Author Manuscript

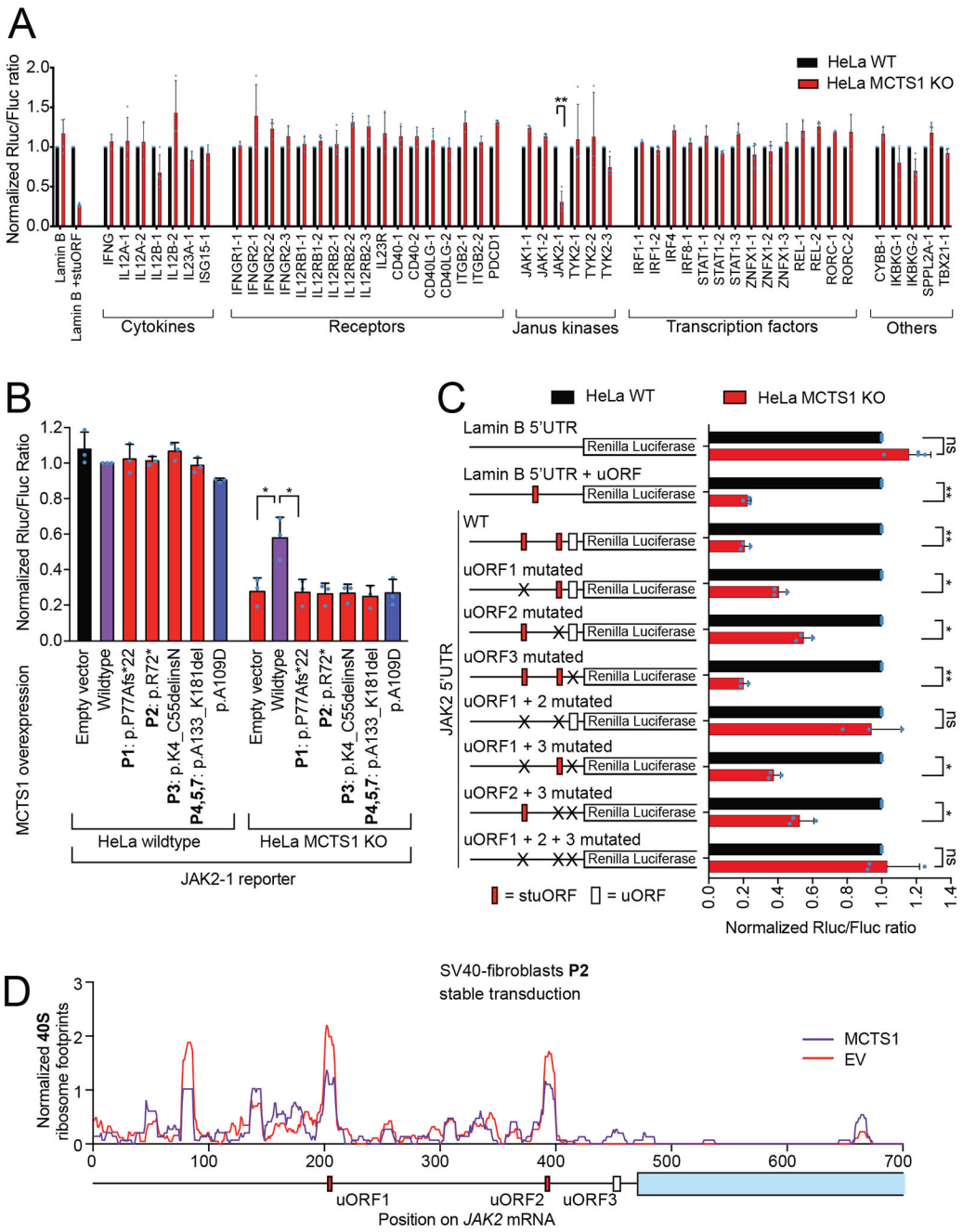


**Figure 4: JAK2 translation depends on MCTS1-mediated reinitiation.**

**(A)** The 5'UTR translation reporters indicated were assessed in WT (black) and MCTS1$^{KO}$ (red) HeLa cells. Number −1, −2 indicate distinct 5'UTR isoforms. Results are shown for 3-5 biological replicates per reporter. Statistical significance was assessed in multiple, two-tailed, unpaired *t*-tests with correction for multiple testing (**$p$<0.005). **(B-C)** Efficiency of JAK2 reporter translation in WT and MCTS1$^{KO}$ cells transfected with the indicated constructs, as assessed in dual-luciferase assays. Results for three biological replicates are shown. Statistical significance was assessed in multiple, two-tailed, unpaired *t*-tests

Author Manuscript Author Manuscript Author Manuscript Author Manuscript

with correction for multiple testing (*$p$<0.05, **$p$<0.005). **(D)** Trace of the 40S ribosome footprints on the endogenous *JAK2* 5'UTR. Red: MCTS1-dependent stuORFs, pink: MCTS1-independent uORF, blue: JAK2 main ORF.

Author Manuscript Author Manuscript Author Manuscript Author Manuscript

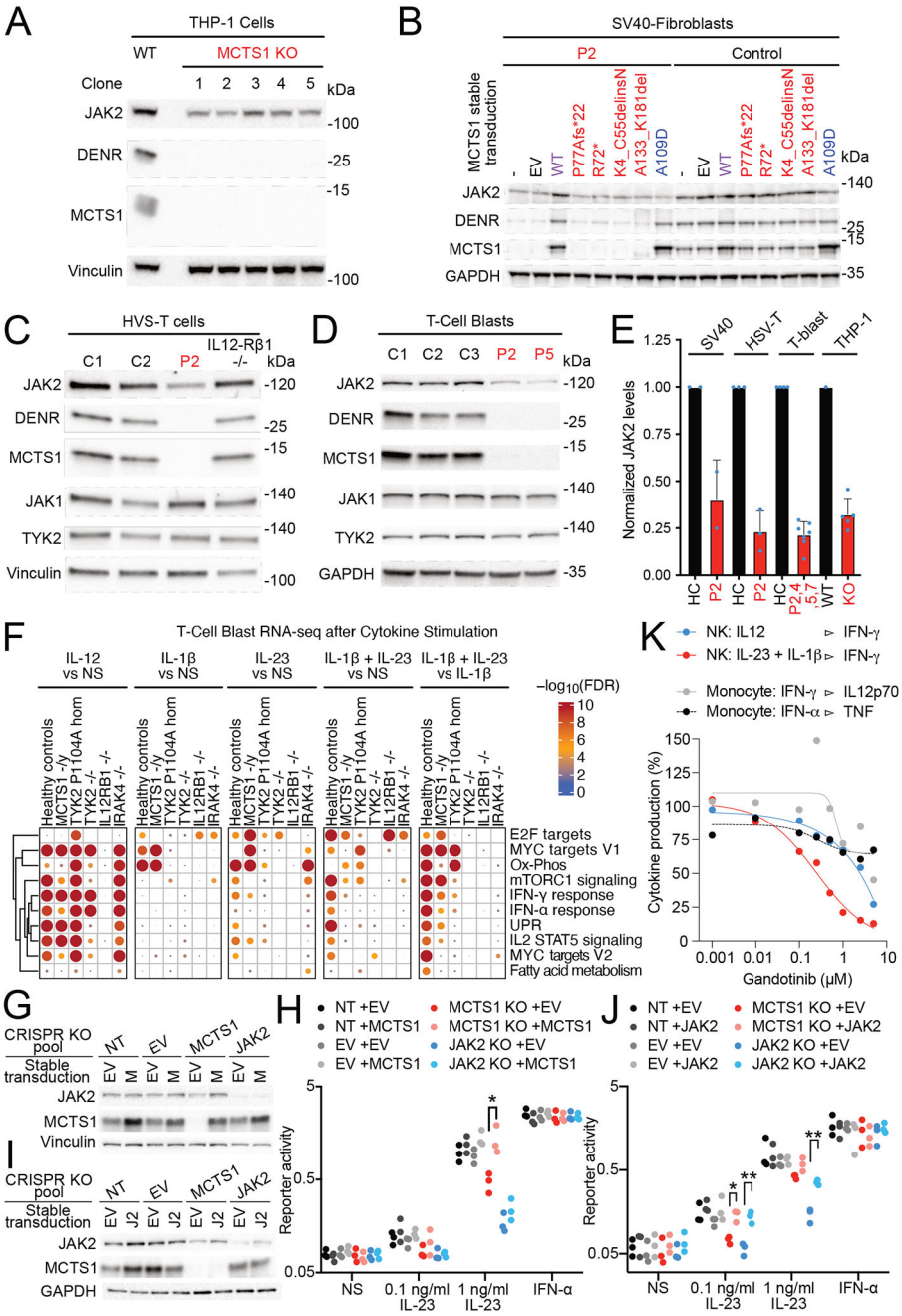


**Figure 5: JAK2 is poorly expressed in cells derived from MCTS1-deficient patients.**

**(A-D)** Western blot for JAK2, MCTS1, DENR and vinculin on total lysate from **(A)** MCTS1$^{KO}$ THP-1 clones (1 to 5) and wild-type (WT) THP-1 cells, **(B)** SV40-fibroblasts from P2 and a healthy control stably transduced with the indicated overexpression constructs, **(C)** HSV-T cells from P2, healthy controls and an IL-12Rβ1-deficient patient and **(D)** T-cell blasts from P2, P5 and healthy controls (C1, C2 and C3). The data shown are representative of three (A, C, D), or (B) two independent experiments.) **(E)** Quantification of JAK2 protein levels relative to a loading control from (A-D) **(F)** Gene set enrichment

Author Manuscript Author Manuscript Author Manuscript Author Manuscript

analysis of RNA-seq analysis of T-cell blasts from heathy controls ($n$ = 9), MCTS1-deficient ($n$ = 4), TYK2-deficient ($n$ = 1), IL-12Rβ1-deficient ($n$ = 1), IRAK4-deficient ($n$ = 1) and TYK2 P1104A-homozygous ($n$ = 2) patients were stimulated with IL-1β (24 h) and with IL-12 and IL-23 (6 h). Dot heatmaps are shown for the 10 gene sets for the healthy controls most strongly affected by stimulation with IL-23 + IL-1β relative to IL-1β alone. **(G, I)** Western blots of the indicated HEK-Blue cell lines stably transduced with the indicated lentiviral vectors. The data shown are representative of three biological replicates. **(H, J)** HEK-Blue colorimetric activity of the indicated cell lines stimulated with the indicated cytokines for 20 hours. Data are shown for three biological replicates and statistical significance was assessed in unpaired, two-tailed $t$-tests, *$p$<0.05, **$p$<0.005. **(K)** The effect of gandotinib on the response to IL-23 + IL1-β or IL-12 in NK cells and to IFN-γ or IFN-α in monocytes. Summary plot, see Figure S7O–R for details. The data shown are the means of six biological replicates performed on NK cells and monocytes from two heathy donors each.

Author Manuscript Author Manuscript Author Manuscript Author Manuscript

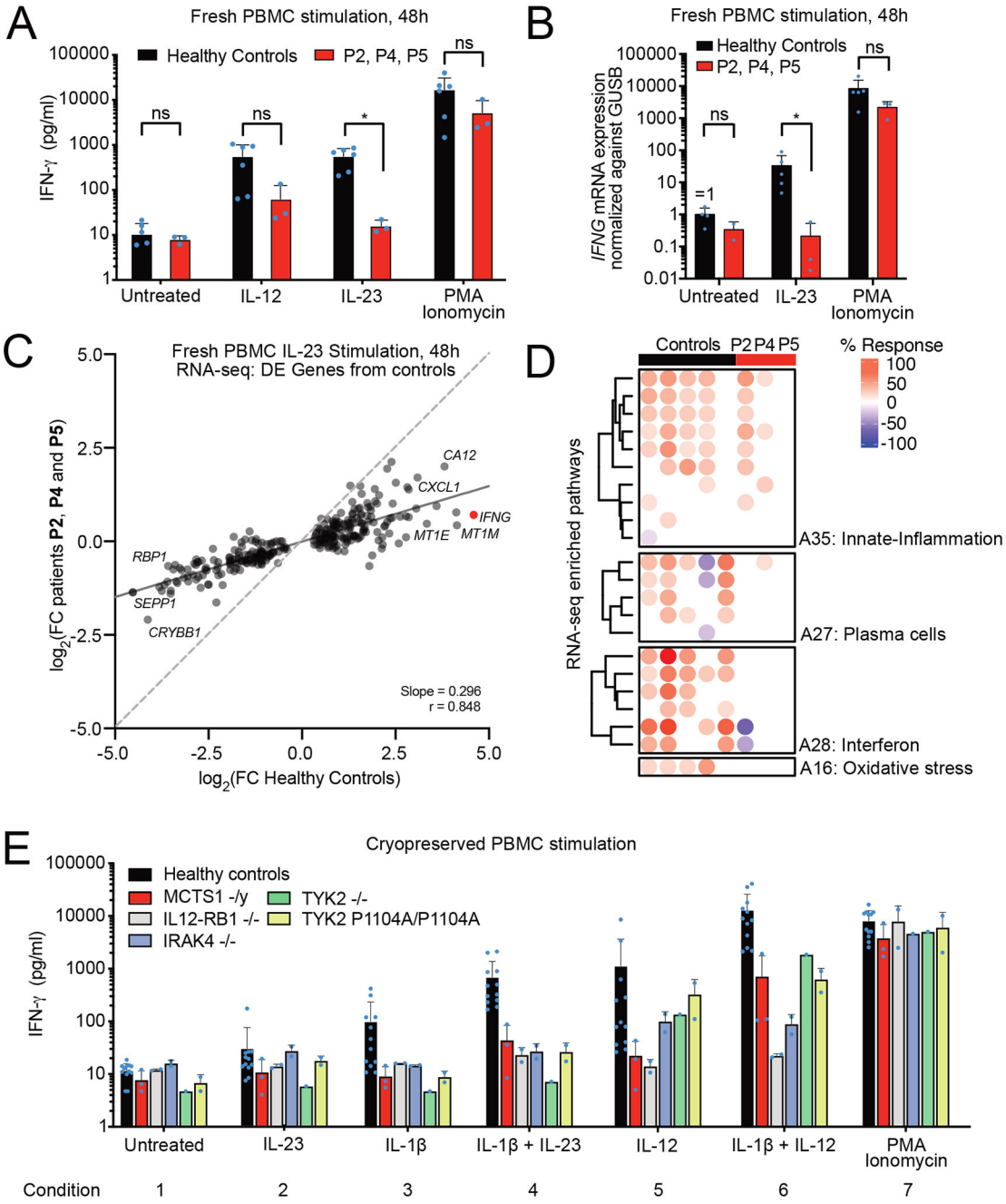


**Figure 6: Defective IL-23-dependent IFN-γ induction in the patients' primary immune cells**

**(A-B)** Fresh PBMCs were stimulated with 50 ng/ml IL-12 or 100 ng/ml IL-23 for 48 hours or with PMA plus ionomycin for 24 hours. IFN-γ levels in the supernatant were assessed by LEGENDplex multiplex ELISA **(A)** and *IFNG* mRNA induction was assessed by qPCR **(B)**. Statistical significance was assessed in unpaired Mann-Whitney *U* tests (*$p$<0.05). **(C)** RNA-seq analysis. $Log_2$ fold-change in mRNA levels upon stimulation with IL-23 (100 ng/ml IL-23 for 48 hours) for transcripts differentially expressed in healthy controls, for the healthy controls and patients. **(D)** Heatmap showing the proportions of transcripts with

Author Manuscript Author Manuscript Author Manuscript Author Manuscript

changes in expression for indicated modules for the various individuals compared (controls versus P2, P4, P5) relative to baseline values in the absence of stimulation. Red: transcripts at higher levels than baseline, blue: decrease in transcript levels relative to baseline. **(E)** Cryopreserved PBMCs of the indicated genotypes were stimulated with 50 ng/ml IL-12, 100 ng/ml IL-23, 2.5 ng/ml IL-1β, or a combination of these cytokines for 48 hours, or with PMA + ionomycin for 24 hours. IFN-γ levels in the supernatant were assessed by LEGENDplex multiplex ELISA. Bars indicate the mean and SD.

Author Manuscript Author Manuscript Author Manuscript Author Manuscript

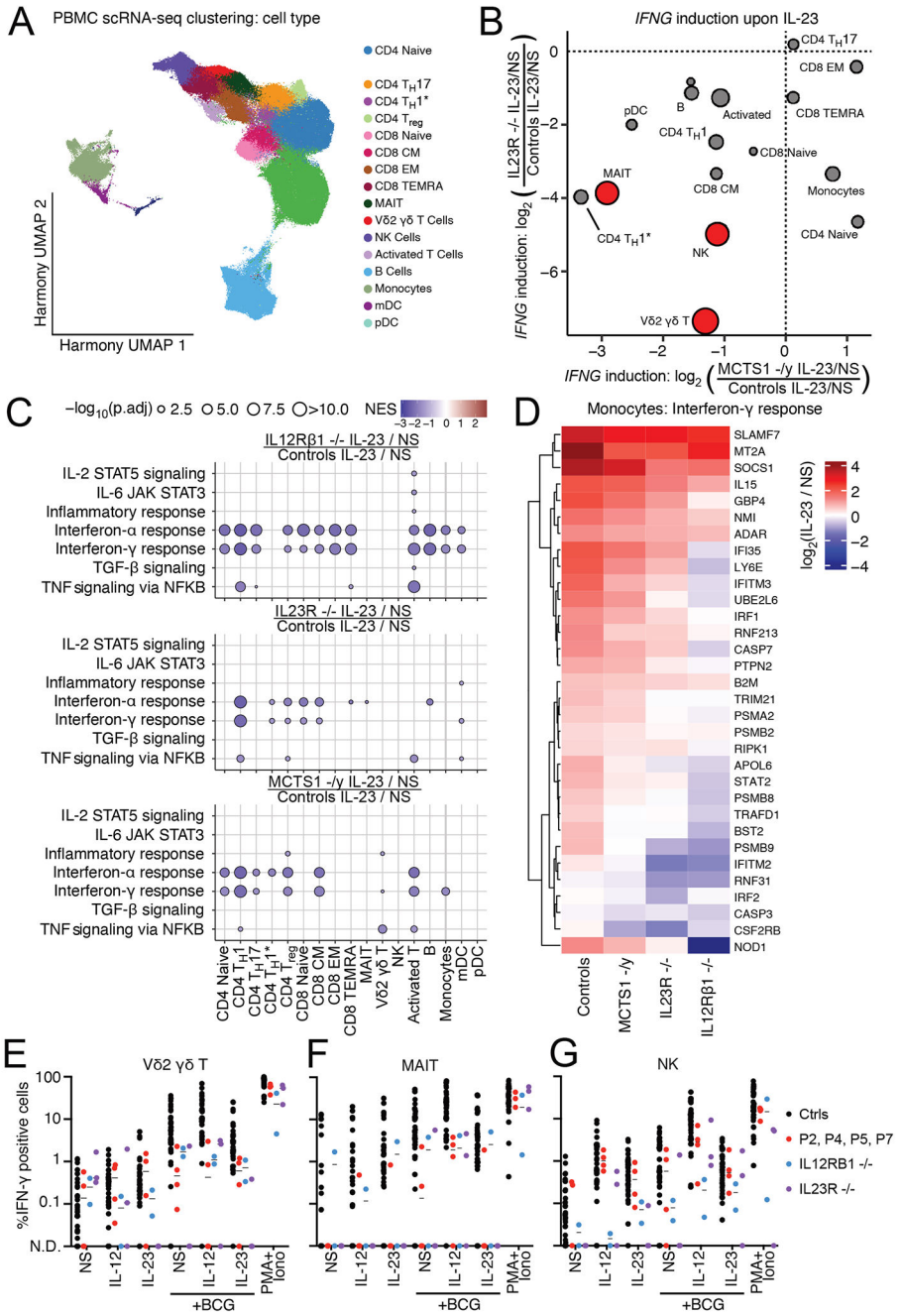


**Figure 7: Patients' Vδ2$^{+}$ γδ T and MAIT cells have impaired *IFNG* induction upon IL-23 stimulation and BCG infection.**

**(A-D)** Single-cell RNA sequencing (scRNA-seq) analysis. PBMCs were either left non-stimulated or were stimulated with IL-23 for 6 hours, and single-cell capture was then performed. **(A)** Clustering analysis identifying 17 major leukocyte subsets. **(B)** The fold-change in *IFNG* mRNA levels following stimulation in MCTS1 patients relative to controls is shown on the *x*-axis. The *y*-axis shows the same parameter for IL-23R$^{-/-}$ patients as a comparison. The size of the circles indicates the median change (IL-23 versus NS) in

Author Manuscript Author Manuscript Author Manuscript Author Manuscript

normalized *IFNG* mRNA levels in controls for the corresponding subset. **(C)** Pathway analysis of the transcriptional response to IL-23 in IL-12Rβ1$^{-/-}$, IL-23R$^{-/-}$ and MCTS1-deficient PBMCs relative to healthy control PBMCs, using the 50 Hallmark gene sets. Results are shown for selected immune-related gene sets. NES, normalized enrichment score. **(D)** Leading-edge genes for the Hallmark IFN-γ response gene set common to IL-12Rβ1-, IL-23R-and MCTS1-deficient patients relative to controls are shown. **(E-G)** Induction of IFN-γ in MCTS1-deficient Vδ2$^{+}$ γδ T **(E),** MAIT **(F)** and NK **(G)** cells upon IL-23 stimulation and mycobacterial infection. Frequency of IFN-β-positive Vδ2$^{+}$ γδ T cells following stimulation with cytokine, BCG or PMA plus ionomycin.

Author Manuscript Author Manuscript Author Manuscript Author Manuscript

Key resources table

| REAGENT or RESOURCE | SOURCE | IDENTIFIER |
|---|---|---|
| **Antibodies** | | |
| human MCTS1 | Teleman Lab | N/A |
| human Tubulin | Sigma Aldrich | Cat# T9026, RRID:AB_477593 |
| human DENR | Teleman Lab | N/A |
| human GAPDH | Santa Cruz | Cat# sc-47724 HRP, RRID:AB_627678 |
| human Vinculin | Santa Cruz | Cat# sc-73614 HRP, RRID:AB_1131294 |
| human JAK2 | Cell Signaling Technology | Cat# 3230, RRID:AB_2128522 |
| human JAK1 | Cell Signaling Technology | Cat# 3332, RRID:AB_2128499 |
| human TYK2 | Santa Cruz | Cat# sc-5271, RRID:AB_628419 |
| human pSTAT1 | BD | Cat# 612133, RRID:AB_399504 |
| Human pSTAT3 | Cell Signaling Technology | Cat# 9134S, RRID:AB_331589 |
| Human pSTAT1-PE (pY701) | BD | Cat# 612564, RRID:AB_399855 |
| Human pSTAT4-PE (pY693) | BD | Cat# 562073, RRID:AB_10895804 |
| Human pSTAT3-PE (pY705) | BD | Cat# 612569, RRID:AB_399860 |
| Anti-Human gamma delta TCR – Alexa 647 | BioLegend | Cat# 331214, RRID:AB_1089210 |
| Anti-human CD3 – V450 | BD Biosciences | Cat# 560365, RRID:AB_1645570 |
| Brilliant Violet 605 anti-human CD56 (NCAM) (Clone 5.1H11) | BioLegend | Cat# 362538, RRID:AB_2565856 |
| BUV563 Mouse Anti-Human CD4 Clone SK3 (also known as Leu3a) | BD Biosciences | Cat# 612912, RRID:AB_2870197 |
| Anti-TCR Vδ1-FITC, human | Miltenyi Biotec | Cat# 130-118-362, RRID:AB_2751495 |
| BUV737 Mouse Anti-Human CD8 Clone SK1 | BD Biosciences | Cat# 612754, RRID:AB_2870085 |
| APC/Fire 750 anti-human TCR Vδ2 Antibody | BioLegend | Cat# 331420, RRID:AB_2687326 |
| Brilliant Violet 785 anti-human CD20 [2H7] | BioLegend | Cat# 302356, RRID:AB_2566316 |
| Alexa Fluor 700 anti-human TCR Vα7.2 [3C10] | BioLegend | Cat# 351728, RRID:AB_2566337 |
| MR1-5-OP-RU-tetramer tetramer | NIH tetramer core facility | N/A |
| Anti-TCR Vβ11-APC, human (clone REA559) | Miltenyi Biotec | Cat# 130-108-733, RRID:AB_2653741 |
| BV480 Mouse Anti-Human Invariant NK T Cell | BD Biosciences | Cat# 746788, RRID:AB_2744044 |
| Anti-T-bet Mouse Monoclonal Antibody (PE/Cy7) [clone: 4B10] | BioLegend | Cat# 644823, RRID:AB_2561760 |
| Brilliant Violet 711 anti-human IFN-γ (Clone 4S.B3) | BioLegend | Cat# 502540, RRID:AB_2563506 |
| Brilliant Violet 510 anti-human TNF-α (Clone MAb11) | BioLegend | Cat# 502950, RRID:AB_2565860 |
| PerCP/Cy5.5 anti-human IL-17A [BL168] | BioLegend | Cat# 512313, RRID:AB_961397 |
| Rorγt Mouse anti Human, PE, Clone: Q21 559 | BD Biosciences | Cat# 563081, RRID:AB_2686896 |
| Anti-human CD3 – V450 | BD Biosciences | Cat# 560365, RRID:AB_1645570 |
| BUV563 Mouse Anti-Human CD4 Clone SK3 (also known as Leu3a) | BD Biosciences | Cat# 612912, RRID:AB_2870197 |
| BUV737 Mouse Anti-Human CD8 Clone SK1 | BD Biosciences | Cat# 612754, RRID:AB_2870085 |
| **Bacterial and virus strains** | | |

Author Manuscript Author Manuscript Author Manuscript Author Manuscript

| REAGENT or RESOURCE | SOURCE | IDENTIFIER |
|---|---|---|
| *Mycobacterium bovis* BCG | (Vogt and Nathan, 2011, PMID: 21911939) | N/A |
| Stellar™ cells | Takara | Cat# 636763 |
| **Biological samples** | | |
| Peripheral blood mononuclear cells from indicated individuals | This manuscript | N/A |
| Plasma from indicated individuals | This manuscript | N/A |
| **Chemicals, peptides, and recombinant proteins** | | |
| Recombinant human Interleukin-12 | R&D Systems | Cat# 219-IL-025 |
| Recombinant human Interleukin-23 | R&D Systems | Cat# 1290-IL-010 |
| Recombinant human Interleukin-2 | Gibco, | Cat# PHC0023 |
| Recombinant human Interleukin-4 | R&D Systems | Cat# 204-IL |
| Recombinant human M-CSF | R&D Systems | Cat# 216-MC |
| Recombinant human GM-CSF | R&D Systems | Cat# 215-GM |
| Recombinant human RANKL | Peprotech | Cat# 310-01 |
| FcBlock | Miltenyi Biotec | Cat# 130-059-901 |
| Phorbol 12-myristate 13-acetate | MedChem Express | Cat# HY-18739 |
| Lymphoprep | StemCell | Cat# 07801 |
| Cycloheximide | Santa-Cruz | Cat# sc-3508 |
| DNase I, RNase-free | Thermo Scientific | EN0521 |
| RNase I | Ambion | AM2294 |
| GlycoBlue | Ambion | AM9515 |
| Acid phenol–chloroform | Ambion | AM9722 |
| Formaldehyde 16% | Thermo Fisher | Cat# 28908 |
| DSP | Thermo Fisher | Cat# A35393 |
| Nonidet P40 Substitute | AppliChem | Cat# A1694 |
| Ionomycin calcium salt | Sigma-Aldrich | Cat# I3909-1ML |
| Live/Dead Aqua | Thermo Fisher | L34966 |
| Protamine sulfate | Merck | Cat# P3369-10G |
| Aqua Dead Cell Stain kit | Thermo Fisher Scientific | Cat# L34957 |
| HEK-BlueTM Selection | Invivogen | Cat# hb-sel |
| QUANTI-Blue Solution | Invivogen | Cat# rep-qbs3 |
| **Critical commercial assays** | | |
| SureSelect Human All Exon V6 | Agilent | Cat# 5190-8864 |
| RiboZero TruSeq Stranded Total RNA Library Prep Kit | Illumina | Cat# 20020596 |
| 10X Genomics Chromium chip | 10X Genomics | NA |
| Chromium Single Cell 3’ Reagent Kit (v3 Chemistry) | 10X Genomics | Cat# CG000183 Rev |
| Quick-RNA Micro-Prep Kit | Zymo | Cat# R1051 |
| Super-Script II Reverse Transcriptase | Thermo Fisher Scientific | Cat# 18064014 |
| Agilent RNA 6000 Nano Kit | Agilent | Cat# 5067-1511 |

Author Manuscript Author Manuscript Author Manuscript Author Manuscript

| REAGENT or RESOURCE | SOURCE | IDENTIFIER |
|---|---|---|
| CD14 MicroBeads | Miltenyi | Cat# 130-050-201 |
| Agilent Small RNA Kit | Agilent | Cat# 5067-1548 |
| SMARTer smRNA-Seq Kit for Illumina | Takara | Cat# 635031 |
| TruSeq Stranded mRNA | Illumina | Cat# 20020594 |
| Maxpar Direct Immune Profiling Assay | Fluidigm | Cat# 201334 |
| TruSeq RNA single indexes | Illumina | Cat# 20020492 |
| Superscript II reverse transcriptase | Thermo Scientific | Cat# 18064022 |
| Qubit dsDNA HS Assay Kit | Invitrogen | Cat# Q32851 |
| Agilent High Sensitivity DNA Kit | Agilent | Cat# 5067-4626 |
| pCR™4-T0P0® vector | Invitrogen | Cat# K457502 |
| Dual-Luciferase® Reporter Assay System | Promega | Cat# E1910 |
| Qiagen blood mini kit | Qiagen | Cat# 51104 |
| Lipofectamine 2000 | Thermo Fisher | Cat# 11668019 |
| SureSelect Human All Exon 50 Mb kit | Agilent Technologies | Cat# 5190-6213 |
| Big Dye Terminator v3.1 cycle sequencing kit | Applied Biosystems | Cat# 4337455 |
| iPrep PureLink gDNA Blood Kit and iPrep Instruments | Life Technologies, Thermo Fisher Scientific | Cat# 10552894 |
| TaqMan Fast Universal PCR Master Mix (2X), no AmpErase UNG | Thermo Fisher Scientific | Cat# 4352042 |
| Deposited data | | |
| RNA-seq, single-cell RNA-seq, and RIBO-seq | SRA | PRJNA1004232 |
| Experimental models: Cell lines | | |
| HEK293T cells | ATCC | Cat# CRL-11268, RRID:CVCL_1926 |
| HEK-Blue IL-23 sensitive cells | Invivogen | Cat# hkb-il23 |
| HeLa Cells | ATCC | Cat# CRM-CCL-2, RRID:CVCL_0030 |
| THP1 WT Cells | ATCC | ATCC Cat# TIB-202, RRID:CVCL_0006 |
| THP1 MCTS1 KO Cells | This manuscript | NA |
| Cos-7 | ATCC | ATCC Cat# CRL-1651, RRID:CVCL_0224 |
| HT1080 | ATCC | ATCC Cat# CCL-121, RRID:CVCL_0317 |
| γ2A- fibrosarcoma cells | Boisson-Dupuis et al. PMID: 30578352 | NA |
| Experimental models: Organisms/strains | | |
| NA | NA | NA |
| Oligonucleotides | | |
| MCTS1 Exon2+3 Exon trapping Forward | Thermo Fisher Scientific | gatc gaattcCTCATATTCCTCCCCCTAACC |
| MCTS1 Exon2+3 Exon trapping Reverse | Thermo Fisher Scientific | gatc ggatccCCCATTGTATTCTCAGCACC |
| Exon Trapping SPL3_MCTS1_Locus Sequencing primer | Thermo Fisher Scientific | aattggttgtagcaggtaata |
| MCTS1 Site directed mutagenesis of P3 splicing variant forward | Thermo Fisher Scientific | CCTGTCAAAATAGTCCGATGgtctttgtttttgtctgtgt |
| MCTS1 Site directed mutagenesis of P3 splicing variant forward | Thermo Fisher Scientific | acacagacaaaaacaaagacCATCGGACTATTTTGACAGG |

Author Manuscript Author Manuscript Author Manuscript Author Manuscript

| REAGENT or RESOURCE | SOURCE | IDENTIFIER |
|---|---|---|
| MCTS1 sgRNA1 F | Thermo Fisher Scientific | CACCGGCCTGGGAAGGATACAACAA |
| MCTS1 sgRNA1 R | Thermo Fisher Scientific | AAACTTGTTGTATCCTTCCCAGGC C |
| JAK2 Cloning primer F BamH1 | Thermo Fisher Scientific | GAGAACCCTGGACCTatgggaatggcctgcct tacg |
| JAK2 Cloning primer R Xho1 | Thermo Fisher Scientific | TTTTCTAGGTCTCGAtcatccagccatgttatcc c |
| MCTS1_EXON5+6_P5,7_1-1F | Thermo Fisher Scientific | ggcaacctccaacttttattttg |
| MCTS1_EXON5+6_P5,7_1-1R | Thermo Fisher Scientific | tgagacaagatcgtgccact |
| MCTS1_EXON5+6_P5,7_2-1F | Thermo Fisher Scientific | tgtgtaccctgaatcttgactt |
| MCTS1_EXON5+6_P5,7_2-1R | Thermo Fisher Scientific | gcctcctgagttcaagcaat |
| MCTS1_EXON5+6_P5,7_3-1F | Thermo Fisher Scientific | ctgctaggtctctgctctca |
| MCTS1_EXON5+6_P5,7_3-1R | Thermo Fisher Scientific | ggcacatgggttcttttcagt |
| MCTS1_EXON5+6_P5,7_4-1F | Thermo Fisher Scientific | ctgcacctggtcattactgc |
| MCTS1_EXON5+6_P5,7_4-1R | Thermo Fisher Scientific | gcccaagtgcattccttctg |
| MCTS1_EXON5+6_P5,7_5-1F | Thermo Fisher Scientific | ctcaattatttctccccacccc |
| MCTS1_EXON5+6_P5,7_5-1R | Thermo Fisher Scientific | ttgggaggctgatcacttga |
| MCTS1_EXON5+6_P5,7_6-1F | Thermo Fisher Scientific | gggacatggacctgctttag |
| MCTS1_EXON5+6_P5,7_6-1R | Thermo Fisher Scientific | cttcctttgctcatacctgtgt |
| MCTS1_EXON5+6_P5,7_7-1F | Thermo Fisher Scientific | agactgcctatggagtattagca |
| MCTS1_EXON5+6_P5,7_7-1R | Thermo Fisher Scientific | agacacactgcctgagagaa |
| MCTS1_EXON5+6_P5,7_8-1F | Thermo Fisher Scientific | tgggtagtcatgaacatttcca |
| MCTS1_EXON5+6_P5,7_8-1R | Thermo Fisher Scientific | tgatctcgtggagttgtggt |
| MCTS1_EXON5+6_P5,7_9-1F | Thermo Fisher Scientific | tgttctcagaactctaccacct |
| MCTS1_EXON5+6_P5,7_9-1R | Thermo Fisher Scientific | tccagactaagacgtgcataca |
| MCTS1_EXON5+6_P5,7_10-1F | Thermo Fisher Scientific | tcctcattagcttctgggtgt |
| MCTS1_EXON5+6_P5,7_10-1R | Thermo Fisher Scientific | ccttccctcttactcatctgga |
| MCTS1_EXON5+6_P5,7_11-1F | Thermo Fisher Scientific | agtcactttcaagccaggtg |
| MCTS1_EXON5+6_P5,7_11-1R | Thermo Fisher Scientific | ctcccgggttcatgccac |
| MCTS1_EXON5+6_P5,7_12-1F | Thermo Fisher Scientific | aagtcatgcaaggagatggc |
| MCTS1_EXON5+6_P5,7_12-1R | Thermo Fisher Scientific | cctcggtctctcaaagtgct |
| MCTS1_EXON5+6_P5,7_13-1F | Thermo Fisher Scientific | gtctgtcactcattaaaggcagt |
| MCTS1_EXON5+6_P5,7_13-1R | Thermo Fisher Scientific | gcacggtcttggctcacc |
| MCTS1_EXON5+6_P5,7_14-1F | Thermo Fisher Scientific | gtgcatcaaagtcagcccat |
| MCTS1_EXON5+6_P5,7_14-1R | Thermo Fisher Scientific | gggtgttcttaaagcagggc |
| MCTS1_EXON5+6_P5,7_15-1F | Thermo Fisher Scientific | tcatgagtggggttagggtt |
| MCTS1_EXON5+6_P5,7_15-1R | Thermo Fisher Scientific | gtttcgctcttgttgccca |
| MCTS1_EXON5+6_P5,7_16-1F | Thermo Fisher Scientific | acactctatgcggactcaca |
| MCTS1_EXON5+6_P5,7_16-1R | Thermo Fisher Scientific | gcacaatctcggctcactg |
| MCTS1_EXON5+6_P5,7_17-1F | Thermo Fisher Scientific | tggaacttggggaggcttag |
| MCTS1_EXON5+6_P5,7_17-1R | Thermo Fisher Scientific | tgcatgtgatgatgtatgggg |

Author Manuscript Author Manuscript Author Manuscript Author Manuscript

| REAGENT or RESOURCE | SOURCE | IDENTIFIER |
|---|---|---|
| MCTS1_EXON5+6_P5,7_1-1F | Thermo Fisher Scientific | ggcaacctccaacttttattttg |
| MCTS1_EXON5+6_P5,7_1-1R | Thermo Fisher Scientific | tgagacaagatcgtgccact |
| MCTS1 exon2 genomic locus for knockout forward | Thermo Fisher Scientific | GACATTGGTTTTGTGCTGGACAGA |
| MCTS1 exon2 genomic locus for knockout reverse | Thermo Fisher Scientific | ACCGAGCTTTACACAGACAAAAACA |
| Cloning-MCTS2 F (BamH1 EcoR1 digest) | Thermo Fisher Scientific | TTGGTACCGAGCTCGGACCTATGTTC AAGAAGTTT |
| Cloning MCTS2 R( BamH1 EcoR1 digest) | Thermo Fisher Scientific | ATGGATATCTGCAGAATCATTTATATG TCTTCATG |
| Recombinant DNA | | |
| pCDNA3.1 EV | Thermo Fisher | V79020 |
| pCDNA3.1 MCTS1 | This Manuscript | NA |
| pcDNA3.1 MCTS1 P77AFs | This Manuscript | NA |
| pCDNA3.1 MCTS1 R72* | This Manuscript | NA |
| pCDNA3.1 MCTS1 K4-C55 | This Manuscript | NA |
| pCDNA3.1 MCTS1 A133-K181 | This Manuscript | NA |
| pCDNA3.1 MCTS1 A109D | This Manuscript | NA |
| pCDNA3.1 MCTS1 G24C | This Manuscript | NA |
| pCDNA3.1 MCTS1 I30M | This Manuscript | NA |
| pCDNA3.1 MCTS1 E37D | This Manuscript | NA |
| pCDNA3.1 MCTS1 K46R | This Manuscript | NA |
| pCDNA3.1 MCTS1 C55S | This Manuscript | NA |
| pCDNA3.1 MCTS1 R72K | This Manuscript | NA |
| pCDNA3.1 MCTS1 R83K | This Manuscript | NA |
| pCDNA3.1 MCTS1 I102V | This Manuscript | NA |
| pCDNA3.1 MCTS1 S107G | This Manuscript | NA |
| pCDNA3.1 MCTS1 P119S | This Manuscript | NA |
| pCDNA3.1 MCTS1 E137K | This Manuscript | NA |
| pCDNA3.1 MCTS1 Q140P | This Manuscript | NA |
| pCDNA3.1 MCTS1 A142T | This Manuscript | NA |
| pCDNA3.1 MCTS1 D154H | This Manuscript | NA |
| IFNG 5’UTR Reporter | This Manuscript | NA |
| IL12A-1 5’UTR Reporter | This Manuscript | NA |
| IL12A-2 5’UTR Reporter | This Manuscript | NA |
| IL12B-1 5’UTR Reporter | This Manuscript | NA |
| IL12B-2 5’UTR Reporter | This Manuscript | NA |
| IL23A-1 5’UTR Reporter | This Manuscript | NA |
| ISG15 5’UTR Reporter | This Manuscript | NA |
| IFNGR1-1 5’UTR Reporter | This Manuscript | NA |
| IFNGR2-1 5’UTR Reporter | This Manuscript | NA |
| IFNGR2-2 5’UTR Reporter | This Manuscript | NA |

Author Manuscript Author Manuscript Author Manuscript Author Manuscript

| REAGENT or RESOURCE | SOURCE | IDENTIFIER |
|---|---|---|
| IFNGR2-3 5'UTR Reporter | This Manuscript | NA |
| IL12RB1-1 5'UTR Reporter | This Manuscript | NA |
| IL12RB1-2 5'UTR Reporter | This Manuscript | NA |
| IL12RB2-1 5'UTR Reporter | This Manuscript | NA |
| IL12RB2-2 5'UTR Reporter | This Manuscript | NA |
| IL12RB2-3 5'UTR Reporter | This Manuscript | NA |
| IL23R 5'UTR Reporter | This Manuscript | NA |
| CD40-1 5'UTR Reporter | This Manuscript | NA |
| CD40-2 5'UTR Reporter | This Manuscript | NA |
| CD40LG-1 5'UTR Reporter | This Manuscript | NA |
| CD40LG-2 5'UTR Reporter | This Manuscript | NA |
| ITGB2-2 5'UTR Reporter | This Manuscript | NA |
| ITGB2-3 5'UTR Reporter | This Manuscript | NA |
| PDCD1 5'UTR Reporter | This Manuscript | NA |
| JAK1-2 5'UTR Reporter | This Manuscript | NA |
| JAK1-3 5'UTR Reporter | This Manuscript | NA |
| JAK2-1 5'UTR Reporter | This Manuscript | NA |
| TYK2-1 5'UTR Reporter | This Manuscript | NA |
| TYK2-2 5'UTR Reporter | This Manuscript | NA |
| TYK2-3 5'UTR Reporter | This Manuscript | NA |
| IRF1-1 5'UTR Reporter | This Manuscript | NA |
| IRF1-2 5'UTR Reporter | This Manuscript | NA |
| IRF4 5'UTR Reporter | This Manuscript | NA |
| IRF8-1 5'UTR Reporter | This Manuscript | NA |
| STAT1-1 5'UTR Reporter | This Manuscript | NA |
| STAT1-2 5'UTR Reporter | This Manuscript | NA |
| STAT1-3 5'UTR Reporter | This Manuscript | NA |
| ZNFX1-1 5'UTR Reporter | This Manuscript | NA |
| ZNFX1-2 5'UTR Reporter | This Manuscript | NA |
| ZNFX1-3 5'UTR Reporter | This Manuscript | NA |
| REL-1 5'UTR Reporter | This Manuscript | NA |
| REL-2 5'UTR Reporter | This Manuscript | NA |
| RORC-1 5'UTR Reporter | This Manuscript | NA |
| RORC-2 5'UTR Reporter | This Manuscript | NA |
| CYBB-1 5'UTR Reporter | This Manuscript | NA |
| IKBKG-1 5'UTR Reporter | This Manuscript | NA |
| IKBKG-2 5'UTR Reporter | This Manuscript | NA |
| SPPL2A-1 5'UTR Reporter | This Manuscript | NA |
| TKB21-1 5'UTR Reporter | This Manuscript | NA |

Author Manuscript Author Manuscript Author Manuscript Author Manuscript

| REAGENT or RESOURCE | SOURCE | IDENTIFIER |
|---|---|---|
| **Software and algorithms** | | |
| R | The R Project for Statistical Computing | https://www.r-project.org |
| Custom software for sequencing analysis | Aurelio Teleman (github) | https://github.com/aurelioteleman/Teleman-Lab |
| Uni-form Mani-fold Approximation and Projection (UMAP) | Becht et al. (PMID 30531897) | v.0.3.5 |
| Burrows-Wheeler aligner | Li et al. PMID: 19451168 | V0.7.12 |
| GATK | Van der Auwera, G. & O'Connor, B. Genomics in the Cloud: Using Docker, GATK, and WDL in Terra (1st Edition). (O'Reilly Media, 2020). | N/A |
| VEP (Variant Effect Predictor, Ensemble 37) | Wang et al. PMID: 20601685 | N/A |
| SnpEff-4.1a tools | Cingolani et al. PMID: 22728672 | V4.1a |
| Fastqc | Babraham Bioinformatics | https://www.bioinformatics.babraham.ac.uk/projects/fastqc/ |
| Cutadapt | Martin, M. Cutadapt removes adapter sequences from high-throughput sequencing reads. EMBnet.journal 17, 10–12 (2011). | N/A |
| Bowtie 2 | Langmead & Salzberg PMID: 22388286 | Version 2 |
| SAMtools | Li et al. PMID: 19505943 | N/A |
| BEDtools | Quinlan & Hall PMID: 20110278 | N/A |
| BBmap | sourceforge.net/projects/bbmap/ | N/A |
| DESeq2 | Love et al., 2014 PMID: 25516281 | https://bioconductor.org/packages/release/bioc/html/DESeq2.html |
| Cell Ranger | 10X Genomics | https://support.10xgenomics.com/single-cell-gene-expression/software/pipelines/latest/what-is-cell-ranger |
| STAR (2.6.1d) | Dobin et al. PMID: 23104886 | https://github.com/alexdobin/STAR |
| Seurat R package | Stuart et al., 2019 PMID: 31178118 | https://cran.r-project.org/web/packages/Seurat/index.html |
| Uniform Manifold Approximation and Projection (UMAP) | Becht et al., 2018 PMID: 30531897 | https://cran.r-project.org/web/packages/uwot/index.html |
| SingleCellExperiment | | https://bioconductor.org/packages/release/bioc/html/SingleCellExperiment.html |
| SingleR | | https://bioconductor.org/packages/release/bioc/html/SingleR.html |
| muscat | Crowell et al. PMID: 33257685 | https://bioconductor.org/packages/release/bioc/html/muscat.html)) |
| PLINK | Purcell et al. PMID: 17701901 | N/A |
| logistf | | https://cran.r-project.org/web/packages/logistf/index.html |
| **Other** | | |

| REAGENT or RESOURCE | SOURCE | IDENTIFIER |
|---|---|---|
| NA | | |

Author Manuscript Author Manuscript Author Manuscript Author Manuscript